Modeling the Residual Strength Distribution of Structural GFRP Composite Materials Subjected to Constant and Variable Amplitude Tension-Tension Fatigue Loading

Nathan L. Post

Thesis submitted to the Faculty of the
Virginia Polytechnic Institute and State University
in partial fulfillment of the requirements for the degree of

Masters of Science
in
Engineering Mechanics

Scott W. Case, Co-Chair
John J. Lesko, Co-Chair
Michael Hyer
Surot Thangjitham

December 8, 2005
Blacksburg, Virginia

Keywords: Fatigue, Spectrum, Composite, Residual Strength

Modeling the Residual Strength Distribution of Structural GFRP Composite Materials Subjected to Constant and Variable Amplitude Tension-Tension Fatigue Loading

Nathan L. Post

ABSTRACT

One scheme for reliability-based design that is growing in popularity for civil and naval applications is the load and resistance factor design (LRFD). Our goal in this research is the development of a simulation to predict the remaining strength of structural composites subjected to variable fatigue loading and environmental exposure. The results of this simulation can then be used in LRFD to determine appropriate material factors of safety for engineering design applications. The work so far focuses on modeling the response of the material to fatigue damage only. A general phenomenological modeling approach is described and applied in two experimental studies using E-glass/vinyl ester composite materials. Strength distributions are modeled using Weibull statistics and residual strength is modeled using a strength-life equal rank assumption and a Monte-Carlo style simulation.

The model provides good residual strength distribution fits to constant amplitude fatigue data and worked well for ordered block spectrum loading using a 735,641 cycle, 22 stress level spectrum. However, applying a randomized spectrum produced unexpected results with every specimen failing after 200,000 to 400,000 cycles while the model predicts identical residual strength when compared with the block loading case. This work points to a need for focus on developing a better understanding of load order impacts in design of composite structures based on constant amplitude fatigue tests. A future approach toward more detailed micro-mechanics fatigue damage modeling is suggested to enable better modeling of residual strength of laminates subjected to random loading fatigue.

This research was conducted thanks to support from the National Science Foundation Interdisciplinary Graduate Education Research and Traineeship (Award # DGE-0114346) and the Office of Naval Research (Award # N00014-04-1-0195). Note: The opinions expressed herein are the views of the authors and should not be interpreted as the views of the Naval Surface Warfare Center or the Department of the Navy, nor of the National Science Foundation.

Dedication

To my grandparents, Dan and Frieda Post, because without their prompting and support, I would never have come to do my graduate school work in Engineering Mechanics and Virginia Tech.

Acknowledgments

I gratefully acknowledge the continuing support, inspiration, and direction provided by my advisors Dr. Scott Case and Dr. Jack Lesko, without which this thesis and the papers included would not have been possible. I want to thank my other committee members Dr. Michael Hyer and Dr. Surot Thangjitham for reviewing my thesis. Many thanks to Jason Cain, Theo Theophanis, John Bausano, and Kathryn McDonald who had direct parts in making this research happen, and all the other Material Response Group students who are always available to help out in the lab or with a computer problem. And of course, none of this would be possible without Beverly Williams for handling paperwork, and travel arrangements, Joyce Smith for helping with the Graduate School Paper work, and Mac McCord who has always managed to keep the MTS going and take care of all the other little random things around the lab. Finally, thanks to Florian Riebel for teaching me LaTeX coding this past summer which made compiling this document much easier than it otherwise would have been.

Contents

List of Figures

List of Tables

Chapter 1

Introduction

The body of this thesis contains two papers which summarize research work performed toward development of residual strength prediction tools for structural glass fiber/vinyl ester composites subjected to fatigue. The materials examined are intended for use in civil and navel applications where extensive prototyping and full scale durability testing is often impractical. As a result, a need exists to develop predictive tools for the statistical performance of the materials with time so that statistically based design tools can be employed. The first paper, *Modeling the Remaining Strength of Structural Composite Materials Subjected to Fatigue*, presented in Chapter 3 elaborates on the concept probabilistic design and in particular one method for its implimentaiton: Load and Resistance Factor Design [12]. Accurate modeling of how the residual strength distribution of a material changes with time, loading and environment is critical to the successful implementation of a probabilistic design methodology. This forms the main motivation for the work that follows.

To simplify this problem, the research presented here focuses on tension-tension fatigue loading in the absence of other environmental effects or material aging. The goal is to refine existing phenomenological approaches developed by Reifsnider and Case [25] for modeling fatigue strength degradation and through the use of Monte-Carlo style simulations on a computer, use them to predict the residual strength distribution in the material subjected to an arbitrary loading history.

Chapter 3 covers work to refine statistical simulation of residual laminate strength based on modeling the residual strength of a critical element (the 0° fibers in this case) using the degradation of laminate stiffness to calculate the load on this element as a function of cycles. In Chapter 4, aspects of spectrum loading are considered with experiments including ordered block loading and random loading of the laminate. This second paper, *Residual Strength Prediction of Composite Materials: Random Spectrum Loading*, models the laminate as a single material system rather than looking at the details of a critical element (with equal success to the previous more complex approach) and uses a simplified equal rank assumption when calculating residual strength distribution properties. A short review of

residual strength prediction methods and spectrum fatigue of composites is included in the second paper, while a more detailed review is provided in Chapter 2. Finally, in Chapter 5, general observations and overall conclusions from the research presented are made and the outlook for future research in this area is presented.

Chapter 2

Literature Review

2.1 Historical Perspective on Fatigue Life Prediction

Interest in understanding the fatigue behavior of materials grew out of the railroad and later aircraft transportation industries where components were repeated loaded and unloaded during normal use, resulting in failures at stresses much lower than the initial strength of the component. The fatigue characterization of metals has been defined fairly well over the last century. None the less, even in metallic materials, there is still substantial uncertainty and most design work is performed using empirical fits and phenomenological models rather than basic material theory. Today, life prediction within a decade is typically considered satisfactory and substantial safety factors are required for components that can not be regularly monitored for fatigue degradation and crack propagation [9]. Empirical modeling tools including Goodman diagrams and S-N curves are still commonly used today for fatigue characterization of materials [9].

Use of fiber reinforced polymer (FRP) composites in structural applications (primarily aerospace industries) started in the 1970s. Despite the high cost, these materials were attractive due to the high strength to weight ratio they presented, tailorable properties based on the constituents and lay-up, and good fatigue durability. However, fatigue life is still an important consideration in most applications of FRP composites. Although the damage progression in composites is very different from that of metals, most approaches to modeling fatigue durability in composite materials has followed on the procedures developed for fatigue of metals [4].

One significant problem for fatigue modeling in going from the laboratory to design applications is that fatigue characterization of materials is nearly always carried out at constant amplitude loading (generating S-N plots and Goodman diagrams), while most real world applications involve varied amplitude loading of components, which sometimes occur in regular patterns, but are often random in nature [8]. For design purposes, these loads are usually

characterized by a spectrum of peaks and valleys, although there is often uncertainty in what loads will actually be applied. Because applying spectrum loading in experiments is relatively difficult and costly and typically only applicable to one specific application, methods for life prediction of materials based on constant amplitude fatigue data is a major topic in fatigue research.

The earliest fatigue life prediction tool, that is still in common use today, was developed by M.A. Miner in 1945 and is commonly known as Miner's Rule or the Palmgren-Miner Rule because of previous work by Palmgren that went into shaping this approach [21]:

$$D = \sum_{i=1}^{k} \frac{n_i}{N_i} \tag{2.1}$$

In Equation 2.1, n_i is the number of cycles applied at stress level i, N_i is the number of cycles to failure at constant amplitude fatigue stress i, and failure is predicted to occur when $D = 1$ for a total of k applied stress levels. Many authors including [7],[4],[20] have shown that Miner's rule does not accurately predict spectrum load failure time in metals or composites, and under some loading cases can be dangerously non-conservative. Nonetheless, even today, Miner's Rule is still often used in design applications for fatigue lifetime prediction because of its simplicity and the lack of availability of additional data which would enable more accurate models to be used [32].

In metals, various strain hardening, crack nucleation, and crack growth models have been developed to provide improved fatigue life predictions [9]. Rain-flow analysis and other cycle counting approaches have also improved the predictions for fatigue life under spectrum loading [8]. However, in composites, most authors focus on the refinement and application of various residual strength models where failure is predicted when the residual strength decreases below the applied peak stress.

2.2 Residual Strength Models for Composite Materials and Studies of Spectrum Loading Fatigue of GFRP

One of the earliest studies of variable amplitude loading in glass fiber reinforced epoxy composites and one of only a few that provide experimental data was published by Broutman and Sahu [4] in 1972. These authors point out that the fatigue damage mechanism in FRP composites is different from metals because small cracks will develop throughout the laminate during the life of the composite without growing larger or substantially reducing the strength of the composite until the final stage of fatigue where the entire laminate fractures. In this study, they examined the applicability of Miner's rule to two block tension-tension ($R = 0.05$) fatigue loading. They showed Miner's sum to be reasonable for high loading followed by low (average value of 1.03 at failure) but found it was non-conservative (average value of 0.66 at failure) for low stress amplitude followed by high.

To address this discrepancy, Broutman and Sahu proposed a residual strength based model. This model assumes that the residual strength decreases linearly throughout the fatigue life from the initial strength to the final fatigue failure load at the applied peak stress:

$$\sigma_i^* = \sigma_{UTS}^{i-1} - \left(\sigma_{UTS}^0 - \sigma_i\right) \frac{n_i}{N_i} \tag{2.2}$$

where σ_i^* is the residual tensile strength of the material after cyclic loading at ith stress level, σ_{UTS}^{i-1} is the ultimate tensile strength of the material before being cycles at σ_i, σ_{UTS}^0 is the ultimate tensile strength of the virgin composite, and σ_i is the ith cyclic stress. Broutman and Sahu made the assumption of linear reduction of strength during fatigue at any given load level because from their limited data they were not able to determine how the residual strength actually changed. The other advantage to this assumption is that residual strength and lifetime predictions can be made using only the S-N curve data as in Miner's rule. However, because the failure criterion is in terms of residual strength, the main error made by Miner's rule is avoided and for the two block loading applied by Broutman and Sahu, the predictions of fatigue life were relatively accurate [4].

Hahn and Kim performed an extensive study of the fatigue properties of a quasi-isotropic glass/epoxy laminate in 1976, developing S-N relationship and studying the impact of temperature increase during fatigue [16]. These authors noted the tendency for progressive failure of the laminate during fatigue where the 90° plies would develop cracks, followed by the 45° plies prior to ultimate failure of the laminate due to fatigue. This gradual failure also leads to partial delamination of the composite prior to ultimate failure. These authors calculated the statistical distribution of the strength of the laminate using Weibull statistics [38]. The S-N curve data was fit using both a standard logarithmic relationship and a power law relationship, the latter of which provided slightly better fits. They also compared different loading rates using a "static" fatigue rate of 20 $\frac{\text{lbs}}{\text{sec}}$ for short times as well as 4 Hz and 10 Hz sinusoidal fatigue and found that there was no frequency dependance of the material in this range [16].

Schütz and Gerharz [30] published a paper describing the experimental fatigue results for a carbon/epoxy composite where they looked at the fatigue durability of different unidirectional fiber orientations and a quasi-isotropic laminate under various stress ratios. In addition, they measured stiffness degradation in the composite under fully reversed loading. Finally, they looked at the response to a spectrum loading representative of an aircraft duty cycle. Miner's sum was then used to predict the estimated life of the composite and experimental results seemed to back up this technique within 1 to 2 decades of life, although very little data was actually collected on the spectrum loading so it is difficult to determine if this was a statistically accurate result [30].

Yang and Liu [43] developed a more complex statistical model for residual strength in carbon/epoxy composites subjected to fully reversed fatigue loading in 1977. They used Weibull statistics to model the initial ultimate tensile strength of the composite and incorporated this into a linear model similar to the one used by Broutman and Sahu to find the number of

cycles to failure as a statistical distribution based on the residual strength failure criterion. When compared to experimental results in a quasi-isotropic graphite/epoxy laminate, this residual strength model was very promising for constant amplitude fatigue residual strength tests. It was also used to predict residual strength during periodic overload "proof" testing again produced good results [43]. This suggests that the equal rank strength-life assumption implicit in this type of approach is applicable to these materials. Yang further verified this model in a later paper [40].

Chou and Croman expanded on the concept of a *strength-life equal rank assumption* in their 1978 paper [5] and they also presented a less restrictive model for predicting residual strength distributions which includes additional parameters to better fit data when compared to Hahn and Yang's approaches. The residual strength equation as developed by Chou and Croman takes the form:

$$y^{\alpha} = x_{\gamma}^{\alpha} - \left(x_{\gamma}^{\alpha} - S^{\alpha}\right)^{1-i} \left(n^{\alpha_1}\right)^{i} \tag{2.3}$$

where x_γ is a value that gives a cumulative distribution of static strength of $1-\gamma$, S is the applied stress, n is the fatigue life, α is the initial strength distribution Weibull shape parameter and α_1 is the fatigue life shape parameter. Thus, this model enables curve fitting of the statistical distribution of fatigue life as well as the initial strength distribution. The parameter i is a constant that controls the shape of the residual strength curves. We will see later that this parameter has a similar effect on residual strength to the j parameter used by Reifsnider and Case [25] and in the work presented in this paper. Unfortunately, Chou and Croman did not find enough data in the available literature to determine if their proposed model would accurately fit residual strength curves.

In 1980, Yang and Jones [42] published additional information and verification of their residual strength statistical model for fatigue in composites and provided some data on effect of load sequence in composites. They showed conclusively that Minors rule is incorrect for any low followed by high or high followed by low sequence compared to a residual strength model. Then Yang and Jones made comparisons of their statistical residual strength model to block loaded spectrum tests on $[\pm 45]_{2s}$ graphite/epoxy laminates. In 1983, Yang and Du [41] expanded on this work to include spectrum loading based on aircraft duty flight cycles, and to various R ratios with a quasi-isotropic laminate. Here the results were not as good and experiments resulted in lower than predicted fatigue life under spectrum loading.

Hwang and Han [20] presented a summary of fatigue damage accumulation models in 1986. They compared these models with several they developed and to experimental data, and demonstrated significant improvements over Miner's model without a large number of experimentally determined constants. The damage accumulation concept is essentially an inverse failure description when compared to a residual strength model. In a damage accumulation model, a damage parameter, D, is added cumulatively until failure occurs at $D = 1$ [20].

Adam et al. [2] developed a power law approach to modeling the residual strength of composite laminates and performed curve fitting experiments using carbon, glass and kevlar reinforced materials. These authors showed that normalized residual strength relationships

change shape under different environmental conditions but are relatively constant for different stress levels.

Several authors [39], [44] and [26] have discussed correlation between stiffness reduction and residual strength in laminates and in 1990, Talreja [35] provided a continuum damage model and applied it to composite laminate analysis using the stiffness change as an input. However, beyond fitting the data, little progress was made on this front toward predicting stiffness degradation, and correlation to residual strength or life is usually not consistent. For example, as we will see, there is almost no correlation between stiffness change and life in the case presented in Chapter 3.

Gathercole and Adam et al. carried out an extensive study of the fatigue behavior of a carbon fiber/epoxy laminate under constant amplitude and variable amplitude conditions in [15] and [3]. They discussed a variety of cumulative damage laws for predicting failure under variable loading and, based on their 2 and 4 block repeated loading experiments, found that Miner's linear damage law was satisfactory in tension block loading, but drastically overestimated fatigue life in sequences containing compression blocks. A power law model worked better for the compression loading. These authors also noted that in their experiments, the order of the blocks did not appear to be significant. However, it should be noted that these experiments were performed with a relatively short sequence of blocks that was repeated many times until failure.

Diao, Ye and Mai developed a statistical prediction methodology for fatigue of fiber reinforced composite materials [6]. This prediction relied on the lamina level fatigue strength distributions determined for unidirectional lamina at various angles. Then, using a probabilistic failure criterion the fatigue life distribution of a laminate could be predicted. They applied this to several examples of glass/epoxy laminates. While the mean value predictions were fairly good, the main advantage of this model is that the spread of the data could be calculated, and in most cases, good agreement was found with experimental results falling within the 75% confidence bounds. However, the disadvantage to this approach is that a large amount of fatigue data on unidirectional specimens is required. Diao et al. did not address the issue of variable amplitude fatigue in their study and it is not clear how their approach could incorporate aspect simultaneously because the model they developed was based on fatigue strength rather than residual strength or life fraction [6].

In 1997, Schaff and Davidson presented one of the most widely known recent spectrum composite fatigue papers in [27] and [28]. The first paper, [27], presents a non-linear phenomenological model for residual strength during fatigue. This model is strikingly similar to the one created by Reifsnider and colleges [24] in 1991, which is described in Chapters 3 and 4 and is mathematically identical, although different symbols are used in Schaff and Davidson's version:

$$R(n) = R_0 - (R_0 - S_p)\left(\frac{n}{N}\right)^{\nu} \tag{2.4}$$

where $R(n)$ is the residual strength, R_0 is the initial static strength, S_p is peak stress magnitude, n is the cycles at the applied loading S_p, N is the cycles to failure at that stress and ν is

a residual strength curve fitting parameter. However, in addition to Reifsnider's approach, Schaff and Davidson consider that the strength degradation parameter ν is a function of the stress level. Also, they note that experimentally the frequency with which the load is changed during a spectrum test has an additional effect of degrading the residual strength. Thus, these authors chose to incorporate an additional parameter which they call the "cycle mix factor," to attempt to model the experiments. Schaff and Davidson apply this factor only when the magnitude of the mean stress increases from one block segment to the next. The cycle mix factor is calculated as:

$$CM = C_m R_0 \left[\frac{\Delta S_{mn}}{R(n)} \right]^{\left(\frac{\Delta S_p}{\Delta S_{mn}}\right)^2} \tag{2.5}$$

where ΔS_p and ΔS_{mn} are the change in peak and mean stress, respectively, and C_m is a non-dimensional cycle mix constant to be found experimentally. The cycle mix factor is applied to the residual strength for each applicable fatigue load change as:

$$R(n)^+ = R(n)^- - CM \tag{2.6}$$

To apply their model, these authors used the fatigue data previously generated by Broutman and Sahu [4] in 1972.

In a second paper, Schaff and Davidson [28] examined random spectrum fatigue response using their model with their cycle mix factor approach. Here, they use data from Schultz and Gerharz [31]. They examined different R ratios as well as different mean stresses. While the model appears to be successful, the data available was too limited to make conclusive remarks on the effectiveness of the cycle mix factor.

In 2001, Wahl et al. [37] and [36] presented the most comprehensive composite fatigue spectrum testing program results yet, including over 900 tests on a glass/polyester laminate. The intended application of this data set was for wind turbine design and the spectrum tests included various block loading and a random spectrum tests, all in tension-tension fatigue with $R = 0.1$ and $R = 0.5$. Several residual strength models were compared and a non-linear (curve fit) model identical to the Schaff and Davidson or Reifsnider models was shown to be the best fit. However, Wahl's data set contains enough data at each loading case to show a large degree of scatter, particularly in spectrum loaded residual strength and life data, which makes modeling and verification of models relatively difficult [36]. As in previous spectrum work, Wahl found Miner's sum dangerously inadequate for predicting failure of the composites. Wahl also noted a significant sequence effect between short and long blocks and, like Schaff and Davidson, found that there was additional degradation under frequent load changes. However, no attempt was made to explain or model this finding.

Schön and Blom [29] were interested in the problem of removing the low stress level loads from spectrum to provide reasonable testing times. They showed that this could be an acceptable technique that would not significantly impact the residual strength measured, while drastically reducing the testing time on the order of 50%. This is a technique that

was incorporated in the work presented in Chapter 4, although in that case, enough of the spectrum was removed to increase the residual strength significantly.

The concept of a cycle mix effect was again discussed by Filis et al. [14] in 2004. However, while the method was promising, Filis et al. lacked the data to conclusively determine the cycle mix parameters and verify if such a model really worked as a predictive tool for a totally new loading case.

Thus, the current field of experimental residual strength and spectrum fatigue testing and modeling of FRP composites still leaves a lot of unanswered questions. Some type of cycle mix effect seems to exist in many of the materials tested, but quantifying this effect is difficult and it has not been explained at all from a theoretical perspective. However, under constant amplitude and long block spectrum loading, non-linear residual strength models have shown to be robust for a wide variety of laminates.

Chapter 3

Paper: Modeling the Remaining Strength of Structural Composite Materials Subjected to Fatigue

Modeling the Remaining Strength of Structural Composite Materials Subjected to Fatigue

Nathan L. Post , John Bausano, Scott W. Case and John J. Lesko
Materials Response Group Department of Engineering Science and Mechanics
Virginia Polytechnic Institute and State University, MC 219, Blacksburg, VA 24061, USA

ABSTRACT

One scheme for reliability-based design that is growing in popularity for civil and naval applications is the load and resistance factor design (LRFD). Our goal in this research is the development of a simulation to predict the remaining strength of structural composites subjected to variable fatigue loading and environmental exposure. The results of this simulation can then be used in LRFD to determine appropriate material knockdown factors for use in engineering design applications. The work so far focuses on modeling the response of the material to fatigue damage only. The proposed Monte Carlo-style simulation combines a phenomenological residual strength based life prediction model for composites materials with an empirical stiffness based damage accumulation model. This model is demonstrated using data for two glass reinforced vinyl-ester polymer composite systems. The analysis of these results has led to new insight into how the changes in mechanical properties of these materials exposed to fatigue loading can be modeled.

This paper was presented at the International Conference on Fatigue of Composites *in Kyoto, Japan, September 13-15, 2004 and was submitted for a special issue of the* International Journal of Fatigue. *It was revised in August 2005 and was accepted for publication September 6, 2005.*

3.1 Introduction

Reliability-based design enables engineers to select structural components based on the desired reliability of the structure over its lifespan. One scheme for reliability-based design that is growing in popularity for civil and naval applications is called load and resistance factor design (LRFD). The LRFD procedure uses a limit state defined by the probability distributions of the material strength and applied loads to achieve a design optimized for the desired reliability [12]. In LRFD approach, the area where the probability distribution of the loads overlaps the resistance distribution is related to the risk of failure in the design, depicted in Figure 3.1.

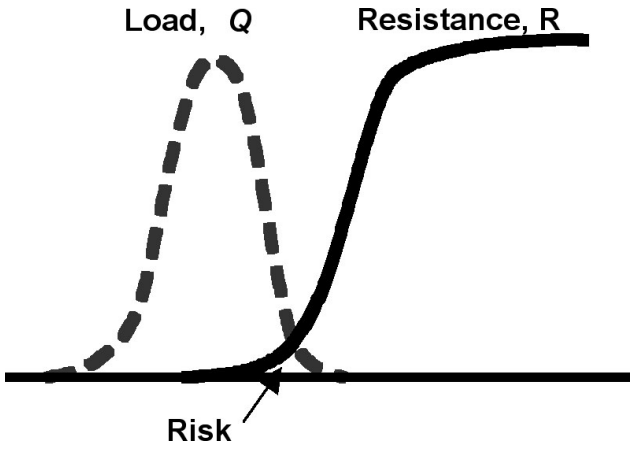

Figure 3.1: Conceptual representation of LRFD

Direct calculation of the probability of failure for each design situation would require design engineers to have a high level of understanding of the statistics and probability calculations involved. It would also be computationally impractical in many situations. Instead, typically LRFD is represented using Equation 3.1, where the design problem has been reduced to a simple inequality involving nominal material properties, loads and resistance and load, factors that can be tabulated for a series of scenarios and probabilities of failure.

$$\phi R_n > \sum \gamma_i Q_{ni} \tag{3.1}$$

In Equation 3.1, R_n is the nominal resistance of the material corresponding to the failure state of interest (typically mean strength or stiffness) and Q_{ni} are the nominal loads applied to the material. The uncertainties in the applied loads are incorporated for a desired reliability using the load factors, γ_i. Engineering design codes will generally fix the load factors for specific situations. The uncertainty of the resistance is described using a resistance "knock-down" factor, ϕ. This resistance factor depends on the particular limit state of interest as well as the material property distribution and failure mode. It is desirable that the

reduction factor take into account the changes in material properties with time so that the nominal resistance can be defined as the initial material strength, independent of load and environmental history. A long history of data and testing over time is available for steel and concrete structures. Design standards provide LRFD reduction factors for these traditional materials [13]. Unfortunately, this history does not exist for the application of new materials such as the fiber reinforced polymer (FRP) composites that are under investigation in this study. Instead, a method is sought to model the resistance distributions in these materials subjected to fatigue and environmental degradation encountered by designs so that the resistance factors may be calculated and tabulated.

The work presented here is an effort to develop and improve the portion of this simulation that determines the material residual strength behavior subjected to a known set of fatigue conditions. The efforts explored in this paper focus on developing analyses to model the remaining strength distribution prior to fatigue failure of relatively inexpensive nearly quasi-isotropic glass-fiber reinforced composites similar to those of interest to naval and civil engineering design. In particular, we are interested in modeling complex composites containing CSM, woven roving plies, etc. By nature, these composites tend to be difficult to analyze using analytical mechanics. Static analysis can be accomplished for woven composites using methods such as the bridging model and finite element analysis as explored by Huang and Ramakrishna [19]. Papanikos et. al. [23] applied a finite element model successfully to fatigue damage of graphite/epoxy quasi-isotropic laminates using an empirical gradual damage accumulation model to reduce the properties of all plies as well as a progressive failure criterion to track the failure of individual plies. However, they did not attempt to include stochastic analysis in this approach. Applying this to analyze stochastic fatigue failure would require detailed descriptions of the distributions of material properties in individual elements. This would be both difficult to characterize for an individual composite and computationally expensive to analyze.

3.2 Methodology

We propose a phenomenological approach to solving reliability problems with these composite materials by developing a model to enable a relatively small number of test results at higher stress levels (lower lifetimes) to be extrapolated statistically to lower stress and longer lifetimes where the material will actually be used. Talreja et al. [34] suggested that the damage accumulation is different for high low and high cycle regimes, with a fatigue limit below which repeated loading does not result in failure. However, the experimental results show continuous S-N curve behavior and the damage accumulation and failure mode are constant over a wide range of stress levels from a few thousand cycles up to several million. Thus, there is no indication of a fatigue limit existing. The approach presented here was originally developed by Reifsnider and colleagues [25] to track fatigue damage in composites using a generalized rate equation for the critical element of the composite that

controls failure. We modify this approach slightly while keeping the general premise. The method used is based on making a distinction between critical and non-critical elements in the composite. The critical elements of the laminate are those whose failure will cause failure of the overall laminate, while the localized failure of non-critical elements simply increases the stress in the critical elements. For the purpose of this initial exploration, we will focus on quasi-isotropic laminates loaded uniaxially in tension and tension-tension fatigue. In the case of axial loading in the 0° direction on these laminates, we can assume that the 0° plies represent the critical elements while the 90 and ±45 degree plies and continuous strand mat (CSM) are non-critical because their failure will not directly cause failure of the composite. It may be much more difficult to identify the critical element in more general laminates such as a $[\text{-}15/+35/\text{-}35/+15/90]_s$ laminate.

We express the remaining strength of the critical element normalized in terms of a failure criterion, Fr, as:

$$Fr(n) = 1 - \left[\int_0^n \left\{(1 - Fa(n))^{\frac{1}{j}} \frac{1}{N(Fa)}\right\} dn\right]^j \tag{3.2}$$

where:

n	Number of cycles
Fa	The normalized maximum load applied to the critical element
Fr	The normalized residual strength of the critical element
$N(Fa)$	Total number of cycles to failure at the applied loading
j	Residual strength fitting parameter

While in the simple constant amplitude tests modeled here, the amplitude of the global stress applied to the composite remains constant during fatigue, the stress on the critical element, Fa, will increase as the non-critical elements become damaged and have reduced modulus.

Non-critical 90°, 45°, and CSM plies experience substantial matrix cracking during fatigue, reducing the overall laminate stiffness in the critical direction and thus increasing the load, Fa, on the critical element as a function of cycles. Fatigue failure occurs when Fa (applied load) becomes greater than Fr (residual strength). Therefore, Fa is a representation of the failure criterion and, in terms of strength, $Fa = \frac{\sigma_{applied}}{X_t}$ where $\sigma_{applied}$ is the applied maximum fatigue stress on the element and X_t is the ultimate strength of the critical element. However, it is difficult to calculate the stress applied to the critical element without detailed information about the geometric and mechanical properties of each component of the laminate as a function of time. Instead, a strain-based failure criterion shown in Equation 3.3 is incorporated that simplifies the analysis and relies only on an empirical representation of the stiffness of the laminate as a function of cycles.

$$Fa(n) = \frac{\epsilon_{applied}(n)}{\epsilon_{failure}} = \frac{\frac{\sigma_{applied}}{E(n)}}{\epsilon_{failure}} \tag{3.3}$$

The strain to failure, $\epsilon_{failure}$, is found from the initial quasi-static strength tests and entered as a random variable for each trial. Implicit in Equation 3.3 is the assumption that $\epsilon_{failure}$

will be constant throughout the fatigue process. This may not be the case for laminates that are not fiber dominated. All that is required to calculate Fa is a model of dynamic elastic modulus during fatigue, $E(n)$. For our purpose here, $E(n)$ will be determined from empirical data. As described by numerous authors [24], FRP composites typically show a modulus decay curve that can be divided into three stages, initial decrease, approximately linear reduction, and final failure, as shown in Figure 3.2. For the purpose of this model, only stage I and II will be represented. This is done to avoid difficulties with modeling stage III as a function of cycles because of the large variability in lifetimes. Because we are interested in predicting remaining strength prior to final failure of the composite, neglecting stage III should not be very significant in the results.

The number of cycles to failure as a function of the instantaneous value of the failure criterion, $N(Fa)$, is modeled using the critical element stress strain curve $N = A + B\log(Fa)$. The constants A, B and the overall rate parameter j are fit such that the simulation will give a best fit of the experimental median values of laminate fatigue life at each stress level and remaining strength point tested using median value properties for inputs.

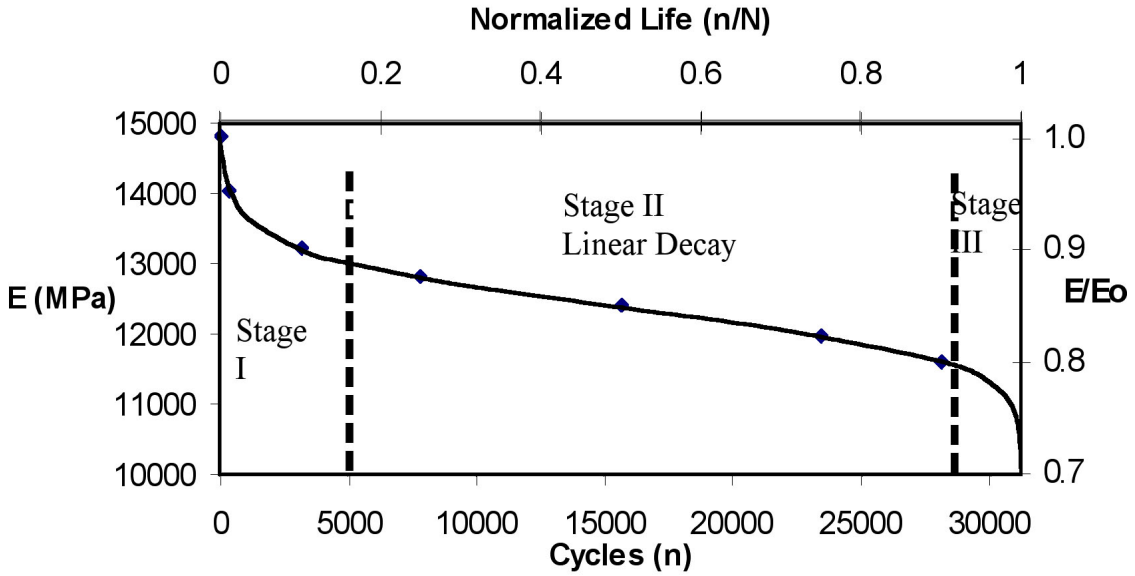

Figure 3.2: Generalized stiffness reduction curve for quasi-isotropic composite material represented in absolute and normalized values

In the simulation, Equation 3.2 is integrated numerically at each cycle by iteratively calculating Fa and $N(Fa)$ and determining the incremental change in the remaining strength of the composite sample. The residual strength can be found by multiplying the initial strength of the composite by Fr. A Monte-Carlo style simulation that incorporates random initial material properties is used to find the resulting remaining strength distribution after a given number of cycles. Extensive testing of glass reinforced vinyl-ester polymer composite systems

is performed to assess the preliminary simulation and the analysis of experimental results has led to new insight into how the changes in mechanical properties of these materials during the fatigue life can be modeled. The simulation incorporates this empirical knowledge and we then compare the resulting calculated remaining strength distribution that to the experimental remaining strength test results.

3.3 Experimental

To validate this modeling approach, tension fatigue tests have been run on two different composite materials. Both materials are similar in that they use E-glass fibers and vinyl ester resin, however, the differences in the type and orientation of fibers, matrix material and manufacturing method yield materials with significantly different mechanical tension fatigue properties.

The first material was a quasi-isotropic pultruded E-glass/Dow Derakane Momentum 640-900 vinyl ester epoxy resin composite laminate provided by Dow Chemical. The laminate lay-up consisted of $[\text{CSM}/0/90/\text{CSM}/\pm 45/\text{CSM}]_s$, where CSM denotes a continuous strand mat. The Dow Derakane Momentum 640-900 matrix used contained 30% styrene and was combined with ASP 400 clay filler. The maximum die temperature was nominally about 166℃ and the material was pulled through the die at a speed of $70\frac{\text{cm}}{\text{min}}$. This produced a continuous strip of material 17.8 cm wide and 0.4 cm thick. Subsequent to the pultusion, the material was cut into 53 cm long segments. These panels remained in the lab for two years and were then heat treated at 170℃ for 2 hours to ensure that the material cure state would remain constant throughout the testing that took place during 2003.

The second material tested is a "pseudo quasi-isotropic" laminate manufactured by Northrop Grumman using vacuum assisted resin transfer method (VARTM). The laminate consisted of 10 layers of Vetrotex 324 woven roving. This fabric has a 5:4 bias in the warp direction and the layup (denoted by warp direction in each layer) was $[0/+45/90/\text{-}45/0]_s$. The matrix used was Dow Derakane 510A vinyl-ester resin (30% styrene). The resulting material was about 0.6 cm thick with one smooth side (against glass mold during manufacture) and one slightly rougher side (compressed by bag). The material was stored for approximately 6 months at room temperature and then subjected to a 4 hour heat treatment at 82℃ to ensure thermal and cure state stability throughout the testing during the summer of 2004.

Each material was manufactured into nominal 2.5x15 cm samples with the long direction corresponding to the 0 direction fibers. Testing took place using 20 kip MTS servo-hydraulic load frames. Strain was measured using a 2.54 cm gauge length extensometer during all strength and fatigue tests. The distribution of initial quasi-static stiffness and strength were determined by breaking 20 specimens in tension. Subsequent tension-tension fatigue test with a minimum stress/maximum stress ratio (R) of 0.1 and a frequency of 10 Hz. was used for all fatigue tests. The dynamic laminate stiffness was tracked for each fatigue sample

during the fatigue process using the peak and valley loads and strains measured by the testing apparatus during each cycle.

For the pultruded material 25 replicates were fatigued to failure at maximum stress levels of 35%, 30% and 25% of the mean ultimate strength (found to be 261 MPa). These stress levels correspond to nominal lifetimes of 35k, 125k and 450k cycles to failure. These results are shown in Figure 3.3. Two remaining strength test points at each stress level were examined, with 15 replicates each, by fatiguing specimens to a specified number of cycles and then breaking the specimen to determine the strength remaining. For the VARTM material, 15 replicates were fatigued at 72%, 52%, 44%, 40% and 36% of the ultimate initial strength (333 MPa), corresponding to nominal lifetimes of 1k, 10k, 50k, 100k and 500k cycles. Additionally, several replicates have been fatigued at 32% (1.5 million cycles). These results are shown in Figure 3.4. Remaining strength tests with 10-15 replicates each have been completed for 5 fractions of lifetime at the 52% and 44% load levels at the cycle locations shown in Figure 3.4.

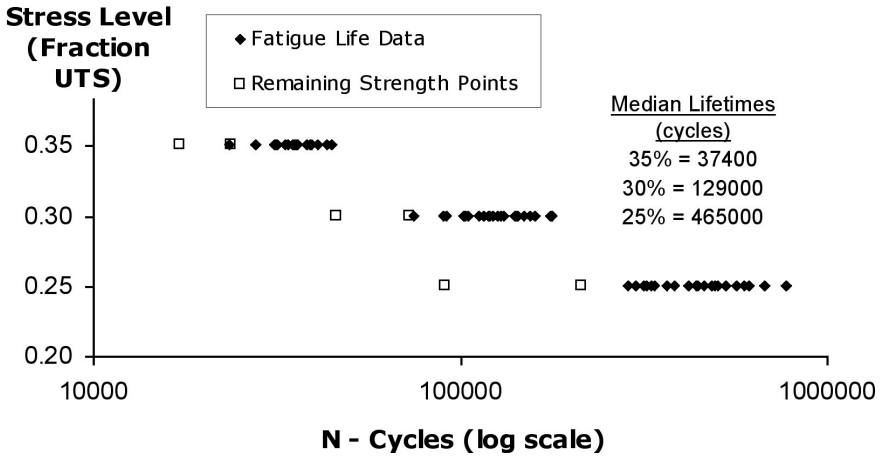

Figure 3.3: Fatigue life data for pultruded material showing remaining strength data collection locations

3.4 Statistical Analysis of Experimental Data

A two parameter Weibull [38] distribution,

$$F(x) = 1 - \exp\left[\left(\frac{x}{\beta}\right)^{\alpha}\right] \tag{3.4}$$

where F is the cumulative density function (CDF), β is the scale parameter (related to the mean), and α is the shape parameter that describes the breadth and shape of the

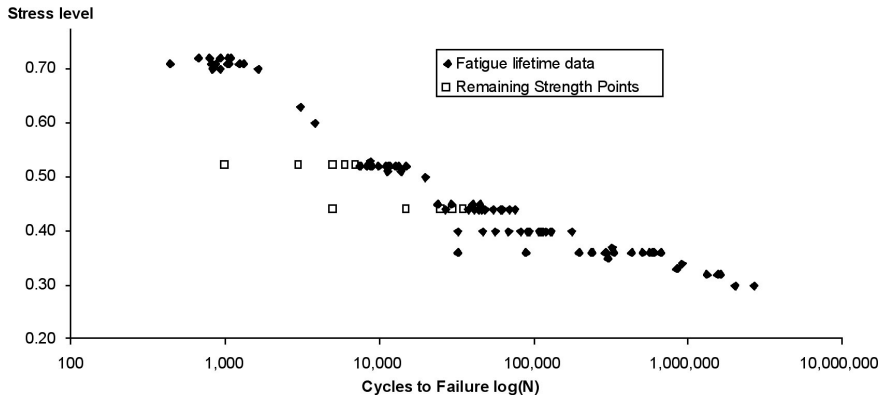

Figure 3.4: Fatigue life data for VARTM material with remaining strength data collection points indicated

distribution, is used to describe the probability distribution of each of the experimental parameters (strength, stiffness, lifetime, etc.). Because of the limited number of samples for each test, there is uncertainty in the calculated α and β values for each distribution. A 95% confidence interval on these values was determined to provide a measure by which to compare them to simulated statistical values. Equations 3.5 and 3.6 give the approximation of the 95% confidence interval for the Weibull distribution that is used [1]:

$$\alpha_{calc} \exp\left(\frac{-0.78 * 1.960}{\sqrt{m}}\right) < \alpha < \alpha_{calc} \exp\left(\frac{0.78 * 1.960}{\sqrt{m}}\right) \tag{3.5}$$

$$\beta_{calc} \exp\left(\frac{-1.05 * 1.960}{\alpha_{calc}\sqrt{m}}\right) < \beta < \beta_{calc} \exp\left(\frac{1.05 * 1.960}{\alpha_{calc}\sqrt{m}}\right) \tag{3.6}$$

In these equations, n is the number of data points used when calculating the distribution values α_{calc} and β_{calc}. Also, for the model to accurately represent the random material properties, we are interested in how the random variable are correlated to each other. The correlation coefficient is calculated as the covariance, $COV(x, y)$, of the random variables, x and y, divided by the product of standard deviations, σ (Equation 3.7). $E[f(x, y)]$ is the expected value of $f(x, y)$ and μ represents the mean value of a random variable.

$$\rho_{xy} = \frac{COV(x, y)}{\sigma_x \sigma_y} = \frac{E\left[(x - \mu_x)(y - \mu_y)\right]}{\sigma_x \sigma_y} \tag{3.7}$$

3.5 Results and Discussion

For the pultruded material, data were collected for 21 initial quasi-static strength tests, each of which produced a stress-strain curve similar to the one shown in Figure 3.5. The

ultimate strength, X_t, and strain to failure, ϵ_f, of each sample was recorded and an initial modulus, E_0, was calculated from the slope of the stress-strain curve between 0.0002 and 0.001 strain. The statistical results of this data are shown in Table 3.1. In addition to calculating the Weibull distribution parameters for each result, the correlation coefficients between the different parameters were also determined. The matrix of these values is shown in Table 3.2. The correlation results indicate that there is relatively little correlation between the strength and stiffness while the stiffness of a sample is negatively correlated ($\rho = -0.85$) to the strain to failure meaning that higher modulus specimens have lower strain to failure.

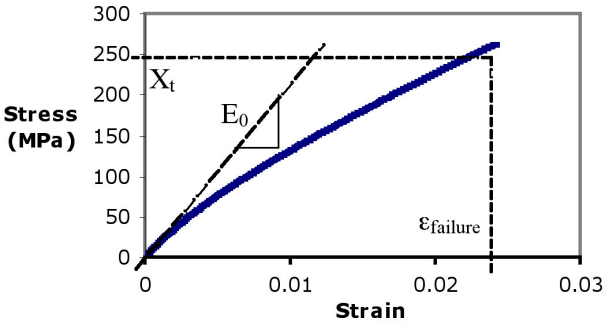

Figure 3.5: Example of quasi-static tensile test result

Table 3.1: Weibull Statistical Results for UTS tests of Pultruded material

	Strength, X_t	Initial Stiffness, E_0	Strain to Failure, ϵ_f
α	47.6	20.0	23.6
β	263 MPa	17.5 GPa	0.0242
Median	261 MPa	17.2 GPa	0.0238

Table 3.2: Correlation Coefficients for Ultimate Tension Strength Data

	X_t	E_0	ϵ_f
X_t	1	0.310	0.149
E_0		1	-0.850
ϵ_f			1

The results for the fatigue tests are plotted in Figure 3.3 and the statistical analysis is summarized in Table 3.3. For each test, the laminate stiffness is tracked during fatigue, resulting in a curve similar to the one shown in Figure 3.2. This data can be analyzed in a number of ways by normalizing with respect to the initial modulus and by normalizing

with respect to the initial modulus E_0 or the cycles to failure N as shown in Figure 3.2. While normalization by lifetime is attractive because it enables inclusion of stage III data into one set of generalized curves, it is not practical for the modeling procedure used because the exact lifetime of a given trial is an unknown. Thus, the stiffness reduction model was developed based on actual cycles rather than normalized life so that it can be used without a predicted time to failure. This choice does limit the ability of the model to simulate the last stage of fatigue degradation close to the failure.

Table 3.3: Fatigue Lifetime Results for Pultruded Data

Load Level	35%	30%	25%
α	5.7	4.4	4.6
β (cycles)	34,300	106,000	509,000

It is desirable to use this stiffness reduction to track damage in the off-axis plies of the composite. The correlation coefficients between the stiffness and normalized stiffness values at different lifetimes along with the initial stiffness and the cycles to failure of each sample are calculated to explore the relationships between these parameters. The full correlation matrix for the 30% load level is shown in Table 3.4. The results for the other two load levels are similar. First, we note that the correlation between initial stiffness, modulus as a function of life and change in modulus as a function of life are generally small ($|\rho| > 0.5$). In addition, these correlations are not consistent from one set of load level data to another. *This shows that stiffness change can not be used directly as a non-destructive measure of remaining life in this material.*

Table 3.4: Correlation coefficient matrix for stiffness degradation data of pultruded material fatigued at 30% of UTS.

	Eo Initital Modulus	E 100 Cycles	E 1000 Cycles	E 10000 Cycles	E 50000 Cycles	E 80000 Cycles	%E 100 Cycles	%E 1000 Cycles	%E 10000 Cycles	%E 50000 Cycles	%E 80000 Cycles
N, Cycles to failure	**-0.330**	**-0.271**	**-0.286**	**-0.294**	**-0.227**	**0.011**	**0.430**	**0.316**	**0.203**	**0.432**	**0.718**
E0, Initial Modulus	1	**0.989**	**0.988**	**0.983**	**0.969**	**0.882**	**-0.176**	**-0.173**	**-0.109**	**-0.141**	**-0.339**
E 100 Cycles		1	0.999	0.995	0.984	0.895	-0.028	-0.032	0.019	-0.038	-0.287
E 1000 Cycles			1	0.997	0.985	0.892	-0.031	-0.020	0.034	-0.027	-0.291
E 10000 Cycles				1	0.987	0.888	-0.018	-0.001	0.077	-0.001	-0.287
E 50000 Cycles					1	0.920	-0.002	0.012	0.079	0.107	-0.196
E 80000 Cycles						1	-0.001	-0.014	0.025	0.140	0.144
%E 100 Cycles							1	0.949	0.852	0.705	0.381
%E 1000 Cycles								1	0.925	0.747	0.352
%E 10000 Cycles									1	0.758	0.289
%E 50000 Cycles										1	0.588
%E 80000 Cycles											1

The magnitude of the stiffness at any time during the life is highly correlated ($\rho > 0.9$) to the initial stiffness. This result is compatible with the assumption that the stiffness of the critical element does not change significantly during the first two stages of fatigue damage because the critical element dominates the bulk stiffness. Thus, the modeled $E(n)$ can be a proportional function of E_0. However, the percent change in modulus (normalized modulus) values are not significantly correlated to the initial modulus and must be considered to be functions of additional independent random variables. At this time, the normalized change in stiffness will be considered deterministically as a function of load level and cycles only. This is a simplifying assumption that ignores the spread in the data shown by the error bars in Figure 3.6.

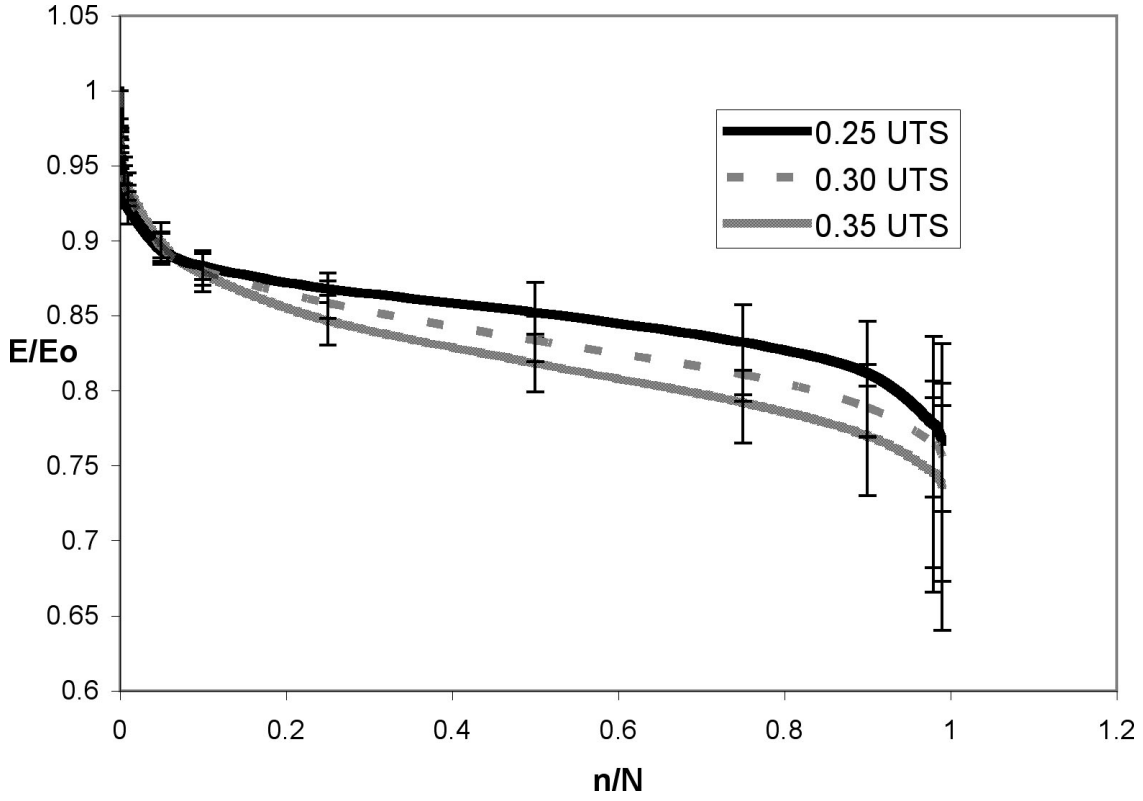

Figure 3.6: Normalized stiffness reduction data. Error bars represent the 10 and 90th percentile of the data

Based on these results and assumptions, we model the stiffness during fatigue as a combination of an exponential decay for stage I and a linear equation for stage II shown in Equation 3.8. This three parameter equation is fit to each measured dynamic stiffness curve by fitting the linear parameters $(1 - a)$ and c to the linear region and then fitting b to the exponential region. Then the median values of a, b and c shown in Table 3.5 are used for each stress level in the model.

$$E(n) = E_0 \left[ae^{-bn} - cn + (1 - a) \right] \tag{3.8}$$

Table 3.5: Median values of stiffness model parameters fit to pultruded data

Load level	a	b	c
35	0.117	$1.18\text{x}10^{-3}$	$3.42\text{x}10^{-6}$
30	0.107	$0.906\text{x}10^{-3}$	$0.933\text{x}10^{-6}$
25	0.109	$0.256\text{x}10^{-3}$	$0.167\text{x}10^{-6}$

Remaining strength tests are performed at each of the six locations indicated in Figure 3.3. By fatiguing 15 specimens at a given stress level to the specified number of cycles, a remaining strength distribution can be calculated. These results are then compared to the distribution of remaining strength predicted by the computer model. One problem that arises when running remaining strength tests is that some samples will fail in fatigue prior to the designated number of cycles. For now, these results have been tracked separately as a percent of samples failing early and are not included in calculating the remaining strength distributions from either the experimental data or the computer model. Unfortunately, this produces a positive bias in remaining strength values because it ignores specimens whose remaining strength falls below the fatigue stress level. This distinction is critical and will have to be addressed prior to using this type of model for design work. However, for the purpose of verification of the model relative to the experimental data, this analysis is acceptable because the specimens that fail early are treated the same way in the model as with the experimental data.

Table 3.6: Median values of stiffness model parameters fit to VARTM data

Load level	a	b	c
52	0.158	$19.4\text{x}10^{-3}$	$11.7\text{x}10^{-6}$
44	0.160	$12.8\text{x}10^{-3}$	$3.76\text{x}10^{-6}$

Computer model results

Using median value results, the model is run iteratively to solve for A, B and j such that the resulting remaining strength values at each remaining strength point and each stress level lifetime are a best least-squares fit. For the pultruded material, the parameters are $A = 0.76$, $B = -0.099$, $j = 0.70$. For each load level and number of cycles, 1000 random trials are generated with initial properties that match the distribution of the experimental material. The program is then run on each trial until the desired number of cycles and the resulting remaining strength for each trial is recorded. From this data, the simulated

remaining strength distribution Weibull parameters, α and β, are calculated. These results are summarized in Figures 3.7 and 3.8. The simulated shape parameters, α, show a positive result with α falling within the experimental 95% confidence interval in every case except for the highest load level with the number of cycles. Note that the confidence intervals on the simulated results are very tight because 1000 virtual trials were used. Thus, these intervals are not shown on the plots to improve clarity. The agreement in distribution shape is very good at the lowest load level (25% of ultimate) which approaches the loads where materials might actually be used in applications. The agreement between the simulated and actual location parameters, β, is less consistent. This is a result of the error introduced when trying to fit the simulation to match the data. Remaining strength points where the median values were close also yield close β values. Thus, perhaps modifications to Equation 3.2 will be required to accurately model these materials.

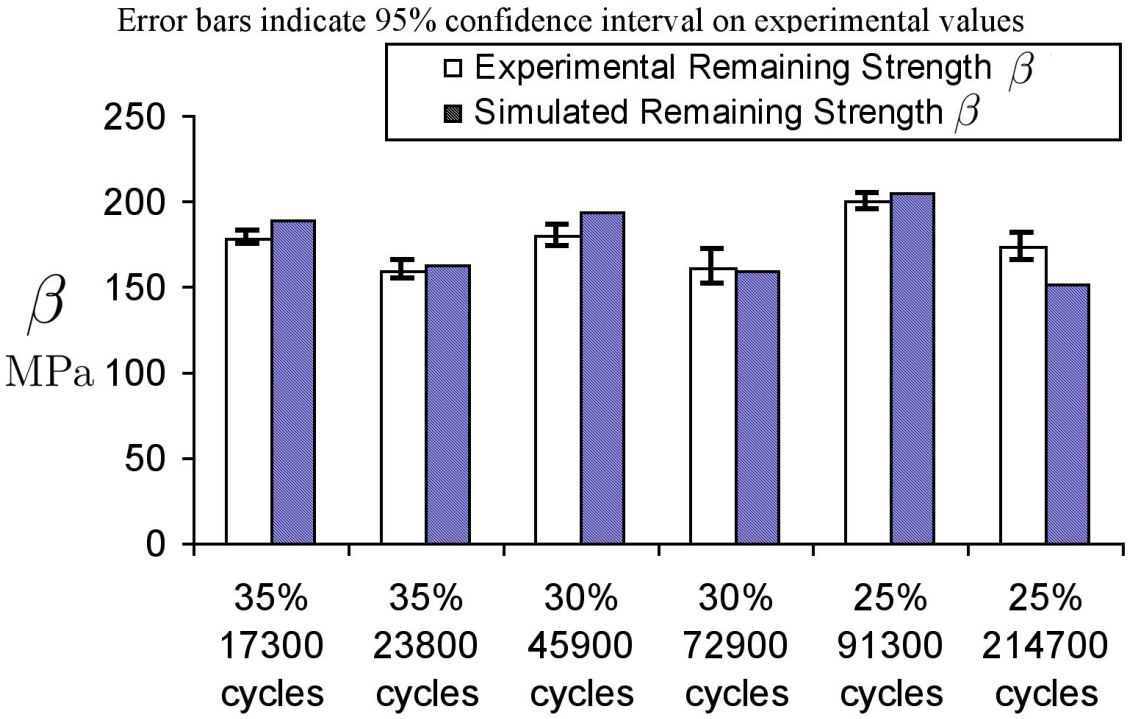

Figure 3.7: Comparison of simulated and experimental remaining strength distribution location parameter, β, for pultruded data

For the case of the VARTM manufactured material, complete data for remaining strength values at two load levels (44 and 52% of the median ultimate strength of 333 MPa) was completed at the time of this publication. The simulation was run in an identical procedure to the pultruded case using the corresponding dynamic stiffness parameters shown in Table 3.6. Median value results at these two load level lifetimes and 5 remaining strength points at

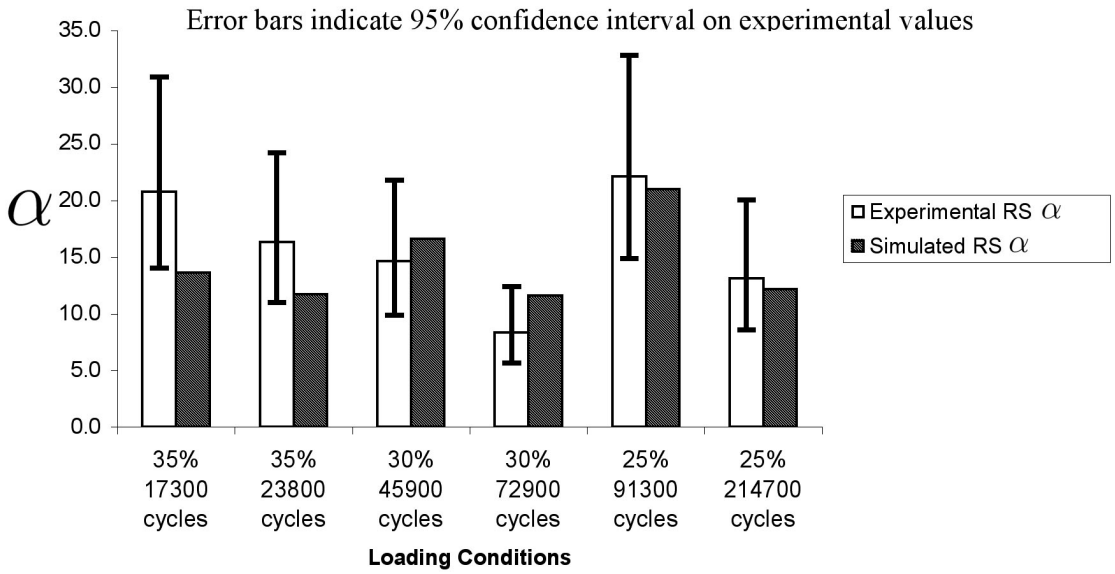

Figure 3.8: Comparison of simulated and experimental remaining strength distribution shape parameter for pultruded data

each load level were used to find $A = 1.07$, $B = -0.12$, and $j = 0.65$. The simulation is then run for 1000 trials that match the statistical distribution and correlation coefficients of the initial experimental material properties for to determine the remaining strength distribution at each lifetime and load level. The numerical distribution parameters are compared in Figure 3.9 and 3.10. Once again, the simulated shape parameters generally fall within the 95% confidence interval of the experimental parameters with the exception of one experimental outlier at 52% loading 5000 cycles. However, it is also worth noting that the model under predicts the shape parameter in almost every case. This error leads to overly conservative designs, but is more acceptable then the model producing too narrower a distribution. Once again, how close the location parameters are is a direct function of how well the median values fit a particular remaining strength point. While generally good, further refinement needs to be made here for the model to accurately represent the experimental data.

3.6 Conclusion

Overall, the results are encouraging with the simulation producing distributions that approximate those found experimentally for two different material systems. While preliminary in nature, this work suggests that there is definite possibility for more generalized statistically based modeling of the response of quasi-isotropic glass fiber/vinyl ester laminates to fatigue damage. Further work is in progress to refine the simulation parameters, include other vari-

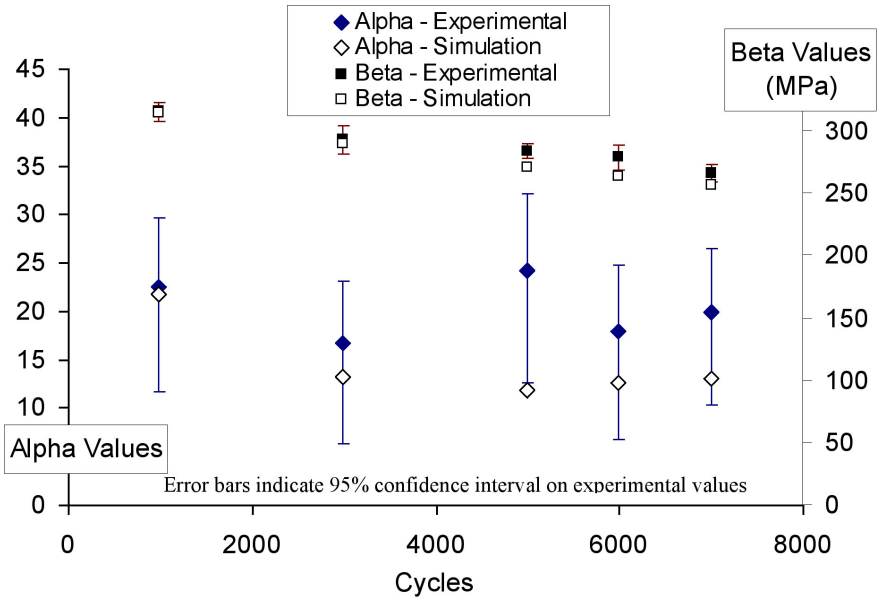

Figure 3.9: Simulated vs. experimental remaining strength distribution parameters for VARTM material at 52% fatigue (nominal 10k cycle lifetime)

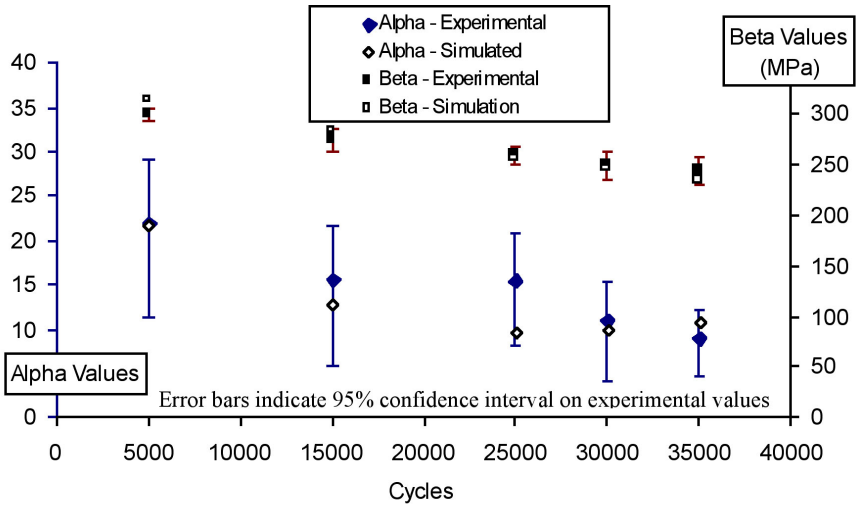

Figure 3.10: Simulated vs. experimental remaining strength distribution parameters for VARTM material at 44% fatigue (nominal 50k cycle lifetime)

ables, study spectrum loading, and verify the simulation method for other material systems. Specifically, the method for determining Fa and the corresponding relationships used to find the dynamic laminate modulus will be addressed and different options will be explored and tested. Eventually, the simulation parameters will be expanded to include other forms of environmental degradation including UV radiation and moisture absorption both of which are known to impact composite performance. These additions will need to be backed up with experimental data to verify the model and the impact of scaling effects needs to be addressed in the modeling process before this method can be used in practical design applications. In addition, further work is required to determine the minimum number and type of tests necessary to achieve accurate predictive results for a material system. Ultimately, the simulation will then need to be applied to specified loading cases and environments to develop a table of LRFD resistance factors that can be used in practical designs. Alternatively, other design techniques such as A-basis and B-basis values could also be found using this type of simulation.

3.7 Acknowledgements

The Authors would like to acknowledge:

Kathryn J. McDonald for her work on the VARTM material data collection and analysis (NSF-REU student).

Office of Naval Research for its support of this work (Award # N00014-04-1-0195). Note: The opinions expressed herein are the views of the authors and should not be interpreted as the views of the Naval Surface Warfare Center or the Department of the Navy.

National Science Foundation IGERT for its financial support (Award # DGE-0114346).

Chapter 4

Paper: Residual Strength Prediction of Composite Materials: Random Spectrum Loading

Residual Strength Prediction of Composite Materials: Random Spectrum Loading

N.L. Post, J. Cain, K.J. McDonald, S.W. Case, J.J. Lesko
121A Patton Hall, MC 219, Virginia Polytechnic Institute and State University, Blacksburg, VA 2460, USA

ABSTRACT

The goal of this project is to identify if and how load order impacts residual strength in an E-glass/vinyl ester composite laminate subjected to variable amplitude fatigue loading. This paper presents results for constant amplitude loading data, which are used to fit parameters for a phenomenological model that can then applied to spectrum loading cases. The residual strength distribution shape, in addition to median values, is modeled using Weibull statistics. Three cases are run experimentally and modeled for a 735,641 cycle spectrum containing 22 different stress levels. The first two are ordered block loading, from highest stress to lowest and from lowest stress to the highest. In both cases, the model predicts the resulting residual strength distribution very accurately. A final case where the entire spectrum was randomized produced unexpected results with every specimen failing after 200,000 to 400,000 cycles while the model predicts identical residual strength when compared with the block loading case. This work points to a dire need for focus on developing a better understanding of load order impacts in design of composite structures based on constant amplitude fatigue characterization.

This paper was presented at the Euromech 473 Colloquium on Fracture of Composites *in Porto, Portugal, October 27-29, 2005 and was submitted for review for a special issue of* Engineering Fracture Mechanics.

4.1 Introduction

In most structural designs where fatigue damage is a concern, materials experiance fatigue loading of various amplitudes throughout their lifetime. Depending on the application, the amplitude and mean values of the loading may have some repeating order or they may be completely randomly ordered. However, fatigue durability characterization of materials is usually performed for constant amplitude loading due to the relative ease of running tests and reporting data, and uncertainty in the real world loads history the material will see. While running a specific variable amplitude loading (spectrum) test might be useful for one application, another set of tests would have to be run for each additional situation. Therefore, the engineering design world requires a method for predicting fatigue life and residual strength of materials under spectrum loading based on constant amplitude fatigue data.

In composite materials, the approach for analysis of variable amplitude fatigue loading has typically followed on the methods used in metals. The earliest cumulative damage model for variable amplitude fatigue is the Palmgren-Miner rule [21]:

$$D = \sum_{i=1}^{k} \frac{n_i}{N_i} \tag{4.1}$$

where D denotes the fatigue damage, n_i is the number of cycles applied at stress level i, N_i is the total cycles to failure at a constant loading amplitude corresponding to i, and k is the number of applied loading levels. Failure is predicted to occur when D=1. The Palmgren-Miner rule is a linear damage model which has seen widespread use in metal fatigue applications and has carried over to composite fatigue despite having been shown to give non-conservative results in some cases. Even given the known problems with this model, it is still used as the baseline against which other variable amplitude fatigue modeling schemes are compared [22].

Van Paepegem and Degrieck [22] provide a literature review on the topic of load sequence effects on the fatigue of composite materials. They found that the published results of different authors and the models they use are inconsistent in determining what type of loading is most damaging. In some loading cases and with some materials, high amplitude followed by low amplitude is shown to be more damaging than low followed by high, while in other cases the reverse is true. However, very little experimental data is actually available to verify these models or to form generalizations. Broutman and Sahu [4] provided one such data set on block loading of cross-ply E-glass/epoxy specimens which indicated that low stress followed by high stress was the more damaging case. This data has been used by several authors to validate their models, including Schaff and Davidson [27] who chose to incorporate a cycle mix factor in their version of a residual strength model. This cycle mix factor attempts to account for the observed additional damage from changing stress levels frequently. Unfortunately, the cycle mix factor must be determined experimentally,

requiring substantial testing for any given material system. In addition, other researchers, including Hwang and Han [20], have found that the reverse effect can be true where high stress followed by low stress amplitude was more damaging.

Van Paepegem and Degrieck also develop their own model, which uses a residual stiffness model where a damage variable is then related to the stiffness [22]. This method lends itself well to the displacement controlled bending tests that these authors examined, but it can not be directly applied to load controlled applications.

Because there is little definitive information, our goal was to exam spectrum fatigue on another material systems where an entire data set could be developed under load controlled testing conditions. In addition, we wish to evaluate the effectiveness of a simple residual strength model, which was found to be reasonably accurate for constant amplitude fatigue in similar systems [25]. We present our findings and data from the current project that examines a pseudo quasi-isotropic E-glass/vinyl ester composite laminate under tensile fatigue by spectrum loading.

4.2 Modeling Procedure

The residual strength phenomenological model we use here is based on previous fatigue modeling work by Reifsnider and Case [25] and takes the form:

$$Fr(n) = 1 - \left[\int_0^n \left\{(1 - Fa(n))^{\frac{1}{j}} \frac{1}{N(Fa)}\right\} dn\right]^j \tag{4.2}$$

where n is the number of cycles, $N(Fa)$ is the number of cycles to failure at a constant amplitude loading Fa, and j is a residual strength fitting parameter. Fa is the normalized peak stress based on the initial unfatigued strength X_t[1] of the specimen:

$$Fa = \frac{\sigma_{applied}}{X_t} \tag{4.3}$$

and Fr is the normalized residual strength

$$Fr = \frac{X_{residual}}{X_t} \tag{4.4}$$

$N(Fa)$ is determined based on constant amplitude fatigue data. In this case, the experimental data fits well to a linear log-log relationship with two parameters:

$$\log(N) = A \log(Fa) + B \tag{4.5}$$

[1]Because the current study only examines tension-tension fatigue, only the tensile strength of the material is considered.

where A and B are fit to the S-N curve data for the material. Thus, this relatively simple model has 3 experimentally determined parameters A, B, and j, which must be fit to fatigue data collected at constant amplitude.

When applied to constant amplitude loading, $Fa = const$, Equation 4.2 reduces to:

$$Fr = 1 - (1 - Fa)\left(\frac{n}{N}\right)^{j} \tag{4.6}$$

For the case of variable amplitude loads, we integrate Equation 4.2 numerically with a step size of 1 cycle for each peak stress applied as shown in Equation 4.7.

$$Fr = 1 - \left[\sum_{k=1}^{n} (1 - Fa_k)^{\frac{1}{j}} \left(\frac{1}{N(Fa_k)}\right)\right]^{j} \tag{4.7}$$

While the model represented in Equations 4.2, 4.6 and 4.7 is designed to calculate residual strength values, it also provides an implicit failure criterion, predicting failure to occur when the residual strength becomes less than the applied stress or $Fr \leqslant Fa$. In addition, we note that this residual strength calculation is independent of loading history order and only depends on the total number of cycles experienced at each stress.

It is desirable to not only model the mean or median residual strength of a material, but also to understand the statistical distribution of strength and how that might change during the fatigue life. To do this, we will take the experimentally measured initial strength distribution and model the residual strength response of specimens from this distribution, finally recalculating the strength distribution resulting in the end. For each initial strength case, Equation 4.7 will be solved numerically for each cycle applied to calculate the final residual strength or time to failure.

The statistical variation in strength is modeled using a two parameter Weibull distribution [38]:

$$F(x) = 1 - \exp\left[\left(\frac{x}{\beta}\right)^{\alpha}\right] \tag{4.8}$$

where $F(x)$ is the cumulative density function, β is the location parameter and α is the shape parameter. Because of the limited number of experimental samples, there will be some uncertainty in the calculated α and β values for each set of results. A 90% confidence interval on α and β was determined to provide a measure by which to compare them to simulated statistical values. The range of this confidence interval can be calculated by [1]:

$$\alpha_{calc} \exp\left(\frac{-0.78 * 1.960}{\sqrt{m}}\right) < \alpha < \alpha_{calc} \exp\left(\frac{0.78 * 1.960}{\sqrt{m}}\right) \tag{4.9}$$

$$\beta_{calc} \exp\left(\frac{-1.05 * 1.960}{\alpha_{calc}\sqrt{m}}\right) < \beta < \beta_{calc} \exp\left(\frac{1.05 * 1.960}{\alpha_{calc}\sqrt{m}}\right) \tag{4.10}$$

where m is the number of data points used when calculating the distribution parameters α_{calc} and β_{calc}.

4.3 Experimental Data Collection

4.3.1 Material System

The material investigated for this study is a psudoquasi-isotropic laminate manufactured by Northrop Grumman using vacuum assisted resin transfer molding (VARTM). The laminate consisted of 10 layers of Vetrotex 324 woven roving. This fabric has a 5:4 bias in the warp direction and the layup (denoted by warp direction in each layer) was $[0/+45/90/-45/0]_s$. The matrix used was Dow Derakane 510A vinyl-ester resin (30% styrene). The resulting material was nominally 0.6 cm thick with one smooth side (against glass mold during manufacture) and one slightly rougher side (compressed by bag). The material was stored for approximately 6 months at room temperature and then subjected to a 4 hour heat treatment at 82 ℃ to ensure thermal and cure state stability throughout the following year of testing. All of the material used in this study was produced at the same time using one batch of fabric and resin. The material was cut into nominal 2.5x15 cm samples, with the long direction corresponding to the 0° direction body coordinate system.

4.3.2 Experimental procedure

Testing took place using 20 kip MTS servo-hydraulic load frames. Strain for modulus calculations was measured using a 1 inch gauge length extensometer during all strength and fatigue tests. The distribution of initial quasi-static stiffness and strength were determined by breaking 20 specimens in monotonic tension using load control with a loading rate of 667 $\frac{\mathrm{N}}{\mathrm{s}}$. Subsequent tension-tension fatigue test were performed with a minimum stress to maximum stress ratio (R) of 0.1 was used for all fatigue tests. The frequency of constant amplitude fatigue tests was maintained at 10 Hz., while spectrum loading tests incorporated a variable frequency between 1 and 10 Hz. to enable the testing equipment to hit all of the highest peaks correctly. In all cases, the fatigue loading waveform was sinusoidal. For the random spectrum loading, a cosine curve was fitted between each maximum and minimum such that the slope of loading the curve was zero at each reversal point.

The dynamic laminate stiffness was tracked for each fatigue sample during the fatigue process using the peak and valley loads and strains measured by the testing apparatus during each cycle as shown in Equation 4.11:

$$E_{dynamic} = \frac{P_{peak} - P_{valley}}{A\left(\epsilon_{peak} - \epsilon_{valley}\right)} \tag{4.11}$$

where P is the applied load, ϵ is the strain and A is the cross section area of the specimen. This essentially results in a calculation of the secant modulus as a function of maximum load since the minimum load for $R = 0.1$ is relatively close to zero. Due to the large amount of data, only a limited selection of data points are plotted from the calculations and results.

In addition, some of the data is averaged over short intervals to remove noise in the strain measurement and make the general trend clear.

4.4 Experimental results

4.4.1 Ultimate Tensile Tests

The initial (unfatigued) tensile strength of 20 specimens resulted in the strength and stiffness values reported in Table 4.1. The median initial strength, $X_t = 334$ MPa, is used for normalization of fatigue stress level (Fa) and residual strength (Fr) throughout the rest of this paper. The initial modulus was calculated based on the slope between from 0 and 0.0002 $\frac{m}{m}$ strain. The final modulus was found over a wider range near failure where the stress-strain curve was visually determined to be approximately linear.

Table 4.1: Statistical summary of quasi-static unfatigued tensile strength for VARTM E-glass/vinyl ester material based on 20 tests

	As recieved Strength MPa	Initial Stiffness GPa	Strain to Failure $\frac{m}{m}$
Mean	333	25.2	0.020
Median	334	25.4	0.019
Weibull α[a]	41.9	19.7	12.8
Weibull β	339	26.0	0.020

[a]Values of α do not have units associated with them.

An example stress-strain curve for the quasi-static tensile test is shown in Figure 4.1. Here, the stress range over which spectrum fatigue cycles take place is indicated. The lowest stress would oscillate between 7.4 and 74 MPa while the highest is between 21.6 and 215 MPa. Because of the curvature of the stress strain plot, the dynamic secant modulus measured will be dependent on stress level.

4.4.2 Constant Amplitude Fatigue

Constant amplitude fatigue tests were performed to find the stress vs. cycles relationship or S-N plot. Stress levels were targeted to for lifetimes of approximately 1000, 10000, 50000, 100000, 500000, and 1500000 cycles. The statistical distribution of lifetimes at each stress level is summarized in Table 4.2.

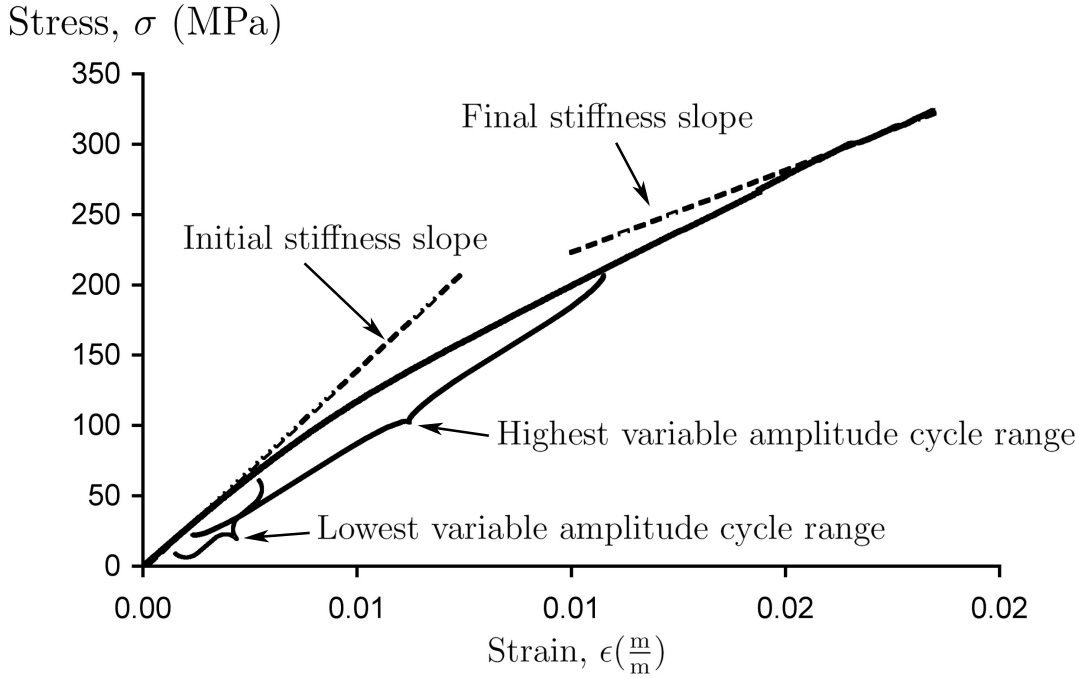

Figure 4.1: Example of stress-strain result for quasi-static tensile test on VARTM E-glass/vinyl ester laminate indicating the initial and final stiffness measurements and the ranges over which dynamic modulus might be calculated.

Table 4.2: Summary of constant amplitude fatigue lifetime results at $R = 0.1$. Fa is the peak cycle stress expressed as a fraction of the median initial strength of 334 MPa

Fa		Lifetime, N (cycles)		
$\left(\frac{\sigma_{applied}}{X_t}\right)$	# of replicates	median	Weibull α	Weibull β
0.71	16	917	3.8	1064
0.52	16	11162	4.3	12517
0.44	16	44010	3.7	50422
0.40	16	109397	4.2	116877
0.36	16	377012	1.4	471390
0.32	3	1542553	-	-

Equation 4.5 is curve fit to the entire 88 sample data set using linear least squares regression. The regression analysis gives $A = -8.7$ and $B = 1.6$, which are two of the parameters required in the remaining strength model described in Section 4.2. This fit, along with the 90% confidence interval is shown on the overall Fa-N plot in Figure 4.2.

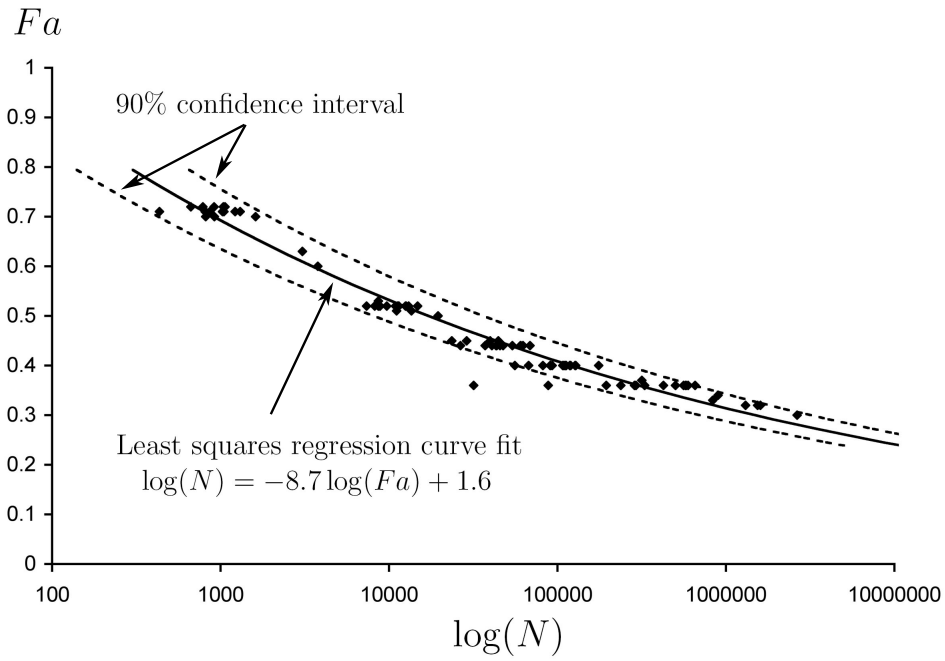

Figure 4.2: Constant amplitude fatigue Fa-N curve for VARTM E-glass/vinyl ester laminate. Fa is the peak cycle stress expressed as a fraction of the median initial strength of 334 MPa and N is the number of cycles to failure.

4.4.3 Residual Strength

Residual strength (RS) tests were performed at 5 points during the life for each of 3 stress levels by loading a specimen at constant amplitude fatigue for a specific number of cycles, then stopping the test and breaking the specimen using the same method as for an ultimate tensile test. The stress levels chosen were 0.52, 0.44 and 0.36 of the median ultimate tensile strength. Cycle counts corresponded to 10%, 30%, 50%,60% and 70% of the target lifetimes for that stress level. Particularly at the longer cycle counts, some specimens failed early and are denoted as premature failures. While not directly included in the analysis, these specimens are important because the residual strength fell below the applied stress prior to reaching the desired number of cycles. In addition, a run out at $Fa = 0.3$ and two at $Fa = 0.25$ were also broken and are treated as additional residual strength tests. The residual strength results are summarized in Table 4.3. Note that the median residual strength and

Weibull parameters in Table 4.3 are calculated based only for the specimens which did not fail prematurely.

Table 4.3: Residual strength data summary for fatigue of E-glass/vinyl ester laminate at $R = 0.1$. Fr is the median residual strength (RS) divided by the median initial strength of 334 MPa

Fa $\left(\frac{\sigma_{applied}}{X_t}\right)$	N	# of premature failures	# of successful tests	median RS (MPa)	Fr $\left(\frac{X_{res}}{X_t}\right)$	Weibull α	Weibull β (MPa)
0.52	1000	0	15	310	0.93	22.3	315
0.52	3000	0	10	292	0.88	16.7	293
0.52	5000	0	15	280	0.84	24.1	284
0.52	6000	2	10	272	0.81	17.8	279
0.52	7000	1	15	264	0.79	19.8	266
0.44	5000	0	15	294	0.88	22.0	299
0.44	15000	0	10	266	0.80	15.7	275
0.44	25000	1	15	249	0.75	15.6	259
0.44	30000	4	10	245	0.73	11.1	249
0.44	35000	4	15	232	0.70	9.1	244
0.36	50000	0	9	275	0.82	18.2	285
0.36	150000	1	10	273	0.82	13.1	277
0.36	250000	1	4	254	0.76	15.4	260
0.36	300000	0	2	221	0.66		
0.36	350000	1	13	232	0.69	8.6	243
0.30	2000000	0	1	235	0.70		
0.25	100000000	2	279	0.84			

Using the median residual strength data and the previously determined A and B constants, the parameter j in Equation 4.2 can now be found. We use Equation 4.6 to calculate a "predicted" RS at each experimentally measured RS point and then j is solved iteratively to achieve the best least-squares fit for the median residual strength at all of these points. In this case, we find $j = 1.16$, which closely matches previous calculations performed by Reifsnider and Case for other glass fiber laminates [25].

4.4.4 Spectrum Loading

For the initial attempt at modeling spectrum loading fatigue, we selected a 99,999,998 cycle spectrum with 30 stress levels based on a 30 year ship lifetime so that the distribution of loads would be somewhat realistic. The spectrum loads were scaled based on the residual strength

analysis presented in Part 4.2 to predict failure at the maximum applied stress level after exactly one time through the spectrum. To obtain reasonable testing times, the spectrum was truncated to the highest 22 stress levels leaving a total of 735,641 cycles after which the residual strength could be measured and compared to model predictions. These fatigue stress levels and corresponding numbers of applied cycles are given in Table 4.4. During the spectrum fatigue tests, an R ratio of 0.1 is maintained for each minimum following a corresponding maximum.

Table 4.4: Spectrum cycle numbers and target stresses

cycles	$\sigma_{applied}$ (MPa)	Fa $\left(\frac{\sigma_{applied}}{X_t}\right)$
337535	74	0.22
182664	81	0.24
98852	88	0.26
53496	95	0.29
28950	102	0.31
15667	109	0.33
8478	116	0.35
4588	123	0.37
2483	130	0.39
1344	144	0.43
727	137	0.41
394	157	0.47
213	150	0.45
115	164	0.49
62	170	0.51
34	177	0.53
18	183	0.55
10	190	0.57
5	196	0.59
3	203	0.61
2	209	0.63
1	216	0.65

The spectrum was applied three ways: first as block loads in ascending order from lowest stress to highest, then as block loads in descending order from highest stress to lowest, and finally, the entire spectrum was randomized so that each individual cycle had an equal probability of occurring at any point during the fatigue. Because there are so many more cycles of the lowest two stress levels than any of the others, the randomized spectrum ends

up looking like a low level fatigue with various higher peaks interspersed as shown in Figure 4.3.

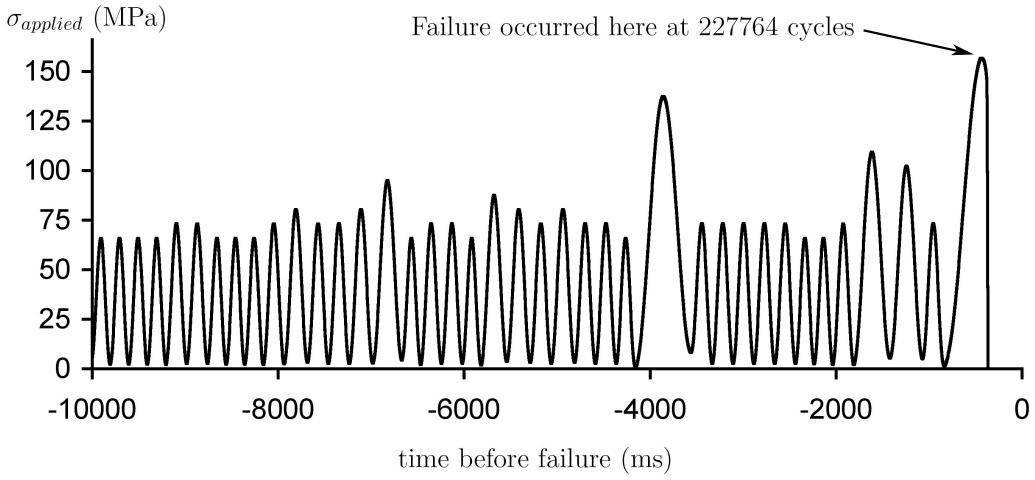

Figure 4.3: Applied loading during the final 10 seconds of life for an example specimen under random spectrum loading.

The experimental data are summarized in Table 4.5. Residual strength for the ascending and descending order block loading tests was statistically identical and none of the specimens failed prior to the end of the test. This suggested to us that loading order was not very significant in determining the residual strength. However, when the randomized spectrum was applied, every specimen broke early between 200000 and 400000 cycles into the spectrum. The waveform stress of the final 10 seconds of some of these tests was recorded so that the final breaking load could be determined. An example of this is shown in Figure 4.3.

Table 4.5: Summary of spectrum loading results

Type of test	# of successful test	# of premature failures	cycles	median RS (MPa)	median Fr
High to Low	11	0	735641	285	0.85
Low to High	13	0	735641	289	0.87
Random	0	12	280149[a]	163[b]	0.49[b]

[a]Median number of random cycles to failure
[b]Based on results from 10 tests where fatigue failure load was recorded

The residual strength analysis was applied to the actual stress peaks applied (rather than the desired peaks in the spectrum). Because the test equipment was not able to hit each peak

perfectly, there is a small difference in the residual strength at the end of the descending block and ascending block spectrum, which in theory should produce identical results because the model is not load order dependent. Comparisons between samples produced very little variation so the predicted result reported is the average result for the loading of all specimens tested for each spectrum block configuration.

Predicted distributions compare very well with the data for both block loading spectrums as shown in Figure 4.4. The simulated and measured distribution parameters are shown in Table 4.6. The predicted values are within the confidence intervals of the experimental data although the predicted distributions of residual strength are wider than the measured distributions (smaller α). However, the predicted residual strength (based on the desired randomized spectrum) for the random spectrum is similar to the block loading and thus the model fails to account for the much more damaging effect of frequently changing the peak load as is the case for the randomized spectrum. Figure 4.5 shows the model predictions for the remaining strength as a function of cycles compared to the data for each of the three spectrum test types performed.

Table 4.6: Spectrum block loading residual strength distribution results. α^+ and α^- are the 90% confidence interval for α and β^+ and β^- are the 90% confidence interval for β in MPa.

	Simulated		Experimental					
Type of test	α	β (MPa)	α^-	α	α^+	β^-	β	β^+
High to Low	13.0	295	12.6	19.9	31.6	293	284	302
Low to High	13.8	298	12.5	19.1	29.2	286	295	304

As an initial step toward investigating the additional damage experienced by the random spectrum laminate, the secant stiffness as a function of cycles was calculated and plotted for example specimens as shown in Figure 4.6. As noted in Figure 4.1, the dynamic secant modulus is dependent on the current fatigue load range and thus is discontinuous for block loading when the stress level changes. In the case of the random spectrum fatigue, the dynamic modulus was only calculated for cycles at the lowest peak stress level and can thus be most directly compared to the lowest block loaded modulus which was applied for almost half the total number of fatigue cycles. In addition, to reduce noise in the data, the modulus was averaged over selected ranges, so the results are qualitative at best. However, they still show a very clear trend of how the stiffness under random loading decreases much more drastically than either block loading scheme, which again points to additional damage occurring from the frequent stress level changes.

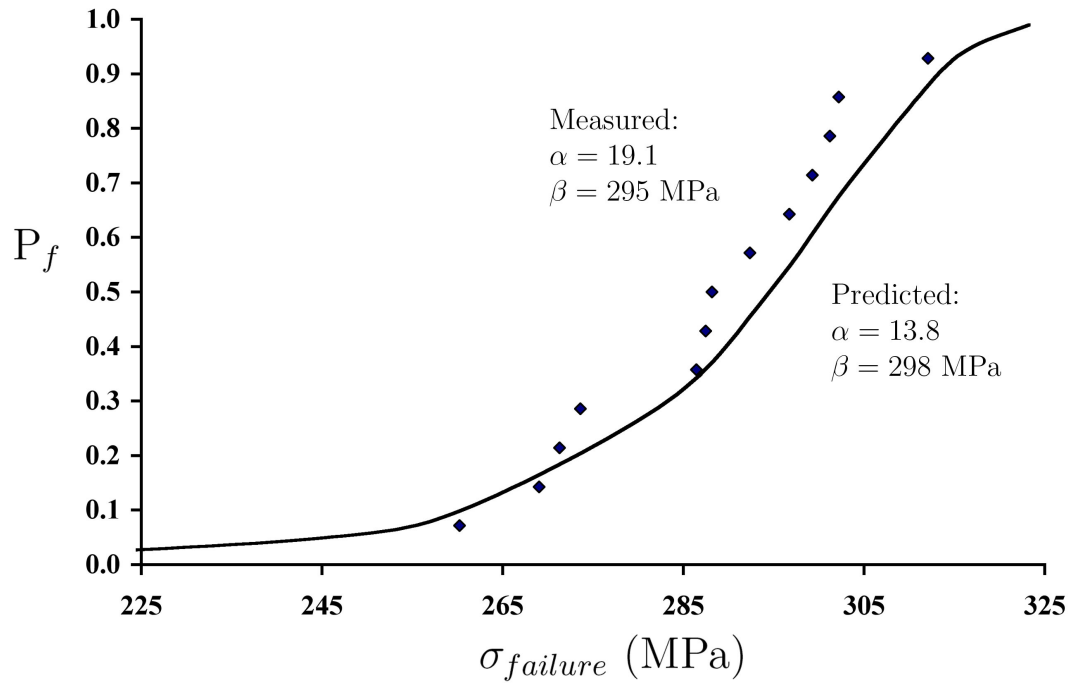

(a) Ascending order block loading spectrum

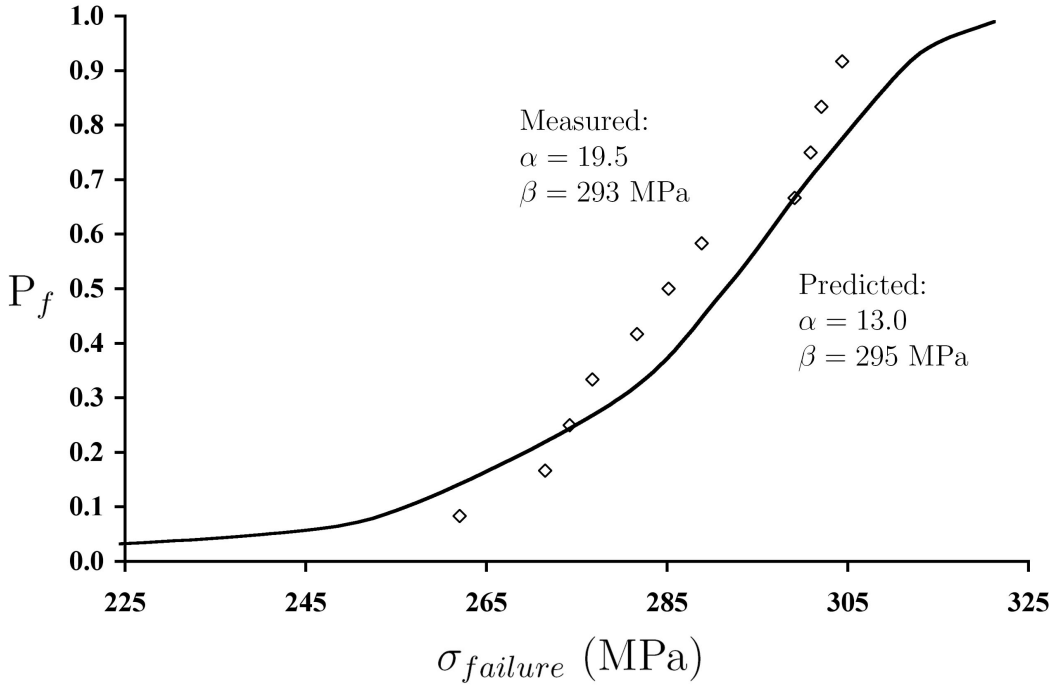

(b) Descending order block loading spectrum

Figure 4.4: Residual strength cumulative probability distribution function comparison for block ordered spectrum experimental and model results

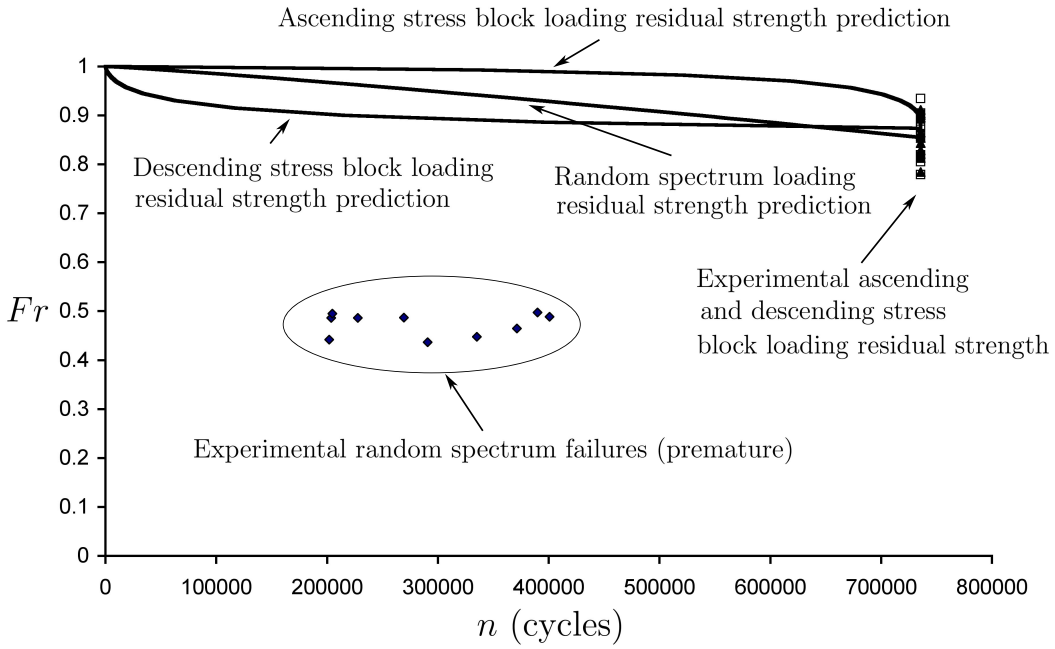

Figure 4.5: Predicted 50 percentile residual strength curves and experimental data for spectrum fatigue tests

4.5 Conclusion

This paper provides a comprehensive fatigue data set on a relatively new structural composite and to provide motivation for further development in our understanding of spectrum fatigue loading of composite materials. The simple residual strength model we propose appeared to be was accurate for constant amplitude loading and worked very well in the case of ordered block spectrum loading where the blocks were relatively large. However, we found experimentally that in this material system, randomized amplitude spectrum fatigue loading is much more damaging than the model indicates. The mechanistic reasons behind this are currently not understood. Some authors have proposed incorporating cycle mix factors or using stiffness data as an indicator, however, neither of these seem to be satisfactory in the general case. Because most material applications involve frequently changing random fatigue amplitudes, understanding the difference between the constant or block loaded amplitude fatigue in the lab and the random spectrum loading response of these composite materials is critical to their safe and successful use in engineering applications.

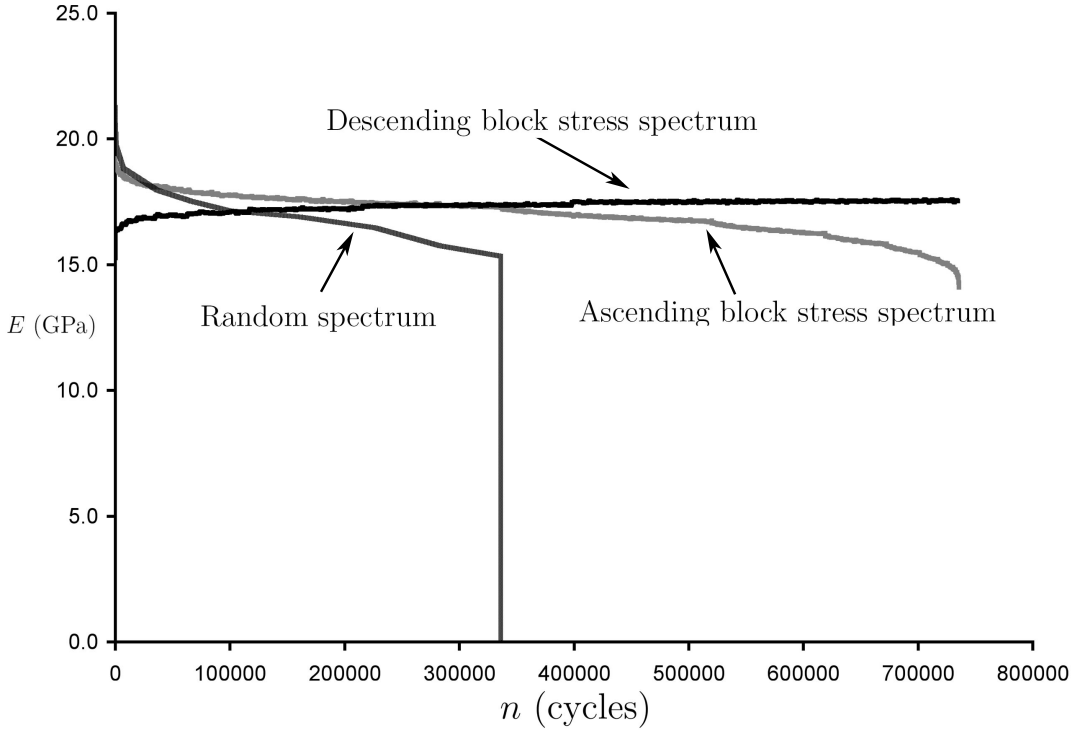

Figure 4.6: Comparison of example dynamic stiffness curves for an ascending block, a descending block, and a random amplitude fatigue test. Note that the discontinuities in the ascending and descending curves correspond to changes in stress level. The random spectrum stiffness was calculated based the lowest stress level cycles only.

4.6 Acknowledgements

Financial support for this study was provided by:

- Office of Naval Research (Award # N00014-04-1-0195). Note: The opinions expressed herein are the views of the authors and should not be interpreted as the views of the Naval Surface Warfare Center or the Department of the Navy.
- National Science Foundation IGERT (Award # DGE-0114346).

4.7 Appendix: Data from experiments

4.7.1 Quasi-static test data

Table 4.7: Quasi-static tensile failure test results for VARTM E-glass/Vinyl Ester Quasi-isotropic laminate

Test #	X_t MPa	$\epsilon_{failure}$ m/m	Initial E GPa	Final E GPa
1	338	0.0207	22.0	13.0
2	342	0.0172	24.6	12.4
3	350	0.0205	24.3	13.1
4	333	0.0202	23.9	14.2
5	321	0.0205	24.7	11.0
6	328	0.0191	24.0	17.6
7	326	0.0196	24.1	13.1
8	353	0.0213	26.9	9.7
9	341	0.0176	27.3	17.6
10	332	0.0189	26.2	14.5
11	343	0.0181	26.9	13.5
12	333	0.0230	25.2	12.2
13	333	0.0207	25.1	11.7
14	327	0.0155	27.6	-
15	323	0.0173	26.6	15.9
16	338	0.0195	25.8	11.7
17	331	0.0192	24.0	13.4
18	332	0.0180	27.1	12.1
19	341	0.0197	25.9	14.4
20	321	0.0202	25.0	12.1

4.7.2 Constant Amplitude Fatigue Data

Table 4.8: Constant amplitude fatigue residual strength results for VARTM E-glass/vinyl ester quasi-isotropic laminate at $R = 0.1$. Fa is peak cycle stress as a fraction of the median initial strength of 334 MPa, n is the number of cycles applied and Fr is the fractional strength remaining

Test #	$\sigma_{applied}$ (MPa)	Fa	N
1	240	0.72	1065
2	240	0.72	665
3	240	0.72	1039
4	240	0.72	785
5	240	0.72	915
6	237	0.71	1222
7	237	0.71	1047
8	237	0.71	1028
9	237	0.71	811
10	237	0.71	814
11	237	0.71	1309
12	237	0.71	864
13	237	0.71	433
14	234	0.70	1612
15	234	0.70	919
16	234	0.70	815
17	210	0.63	3061
18	200	0.60	3784
19	177	0.53	8644
20	174	0.52	8649
21	174	0.52	11249
22	174	0.52	10917
23	174	0.52	8210
24	174	0.52	12559
25	174	0.52	14807
26	174	0.52	12656
27	174	0.52	7355
28	174	0.52	13100
29	174	0.52	11439
30	174	0.52	9711
31	174	0.52	8841

continued on next page

continued from previous page

Test #	$\sigma_{applied}$ (MPa)	Fa	N
32	170	0.51	11076
33	170	0.51	13611
34	167	0.50	19585
35	150	0.45	23577
36	150	0.45	44515
37	150	0.45	39945
38	150	0.45	28848
39	147	0.44	53908
40	147	0.44	60409
41	147	0.44	62321
42	147	0.44	60478
43	147	0.44	68661
44	147	0.44	26530
45	147	0.44	47629
46	147	0.44	43246
47	147	0.44	40838
48	147	0.44	37158
49	147	0.44	43505
50	147	0.44	45549
51	134	0.40	127334
52	134	0.40	108268
53	134	0.40	128291
54	134	0.40	55943
55	134	0.40	119688
56	134	0.40	175401
57	134	0.40	90806
58	134	0.40	118537
59	134	0.40	107562
60	134	0.40	81940
61	134	0.40	112416
62	134	0.40	111176
63	134	0.40	90366
64	134	0.40	110525
65	134	0.40	93131
66	134	0.40	67466
67	124	0.37	316429
68	120	0.36	194930

continued on next page

continued from previous page

Test #	$\sigma_{applied}$ (MPa)	Fa	N
69	120	0.36	329153
70	120	0.36	656262
71	120	0.36	501655
72	120	0.36	579123
73	120	0.36	31848
74	120	0.36	579702
75	120	0.36	286662
76	120	0.36	88014
77	120	0.36	595304
78	120	0.36	292197
79	120	0.36	424870
80	120	0.36	237430
81	120	0.36	560511
82	120	0.36	576533
83	114	0.34	899242
84	110	0.33	834671
85	107	0.32	1542553
86	107	0.32	1601043
87	107	0.32	1309911
88	100	0.30	2644905

4.7.3 Residual strength data

Table 4.9: Constant amplitude residual strength results for VARTM E-glass/vinyl ester quasi-isotropic laminate subjected to fatigue at $R = 0.1$. Fa is peak cycle stress as a fraction of the median initial strength, $X_t = 334$ MPa. N is the number of cycles to failure

Test #	$\sigma_{applied}$ (MPa)	Fa	n	$\frac{n}{N}$	Premature failure	$X_{t,residual}$ (MPa)	Fr
1	174	0.52	1000	0.09		312	0.93
2	174	0.52	1000	0.09		297	0.89

continued on next page

continued from previous page

Test #	$\sigma_{applied}$ (MPa)	Fa	n	$\frac{n}{N}$	Premature failure	$X_{t,residual}$ (MPa)	Fr
3	174	0.52	1000	0.09		285	0.85
4	174	0.52	1000	0.09		334	1.00
5	174	0.52	1000	0.09		309	0.92
6	174	0.52	1000	0.09		310	0.93
7	174	0.52	1000	0.09		311	0.93
8	174	0.52	1000	0.09		278	0.83
9	174	0.52	1000	0.09		301	0.90
10	174	0.52	1000	0.09		316	0.95
11	174	0.52	1000	0.09		331	0.99
12	174	0.52	1000	0.09		318	0.95
13	174	0.52	1000	0.09		309	0.92
14	174	0.52	1000	0.09		318	0.95
15	174	0.52	1000	0.09		292	0.88
16	174	0.52	1000	0.09		318	0.95
17	174	0.52	3000	0.27		280	0.84
18	174	0.52	3000	0.27		300	0.90
19	174	0.52	3000	0.27		292	0.87
20	174	0.52	3000	0.27		257	0.77
21	174	0.52	3000	0.27		251	0.75
22	174	0.52	3000	0.27		300	0.90
23	174	0.52	3000	0.27		296	0.89
24	174	0.52	3000	0.27		279	0.83
25	174	0.52	3000	0.27		293	0.88
26	174	0.52	3000	0.27		297	0.89
27	174	0.52	5000	0.45		278	0.83
28	174	0.52	5000	0.45		290	0.87
29	174	0.52	5000	0.45		293	0.88
30	174	0.52	5000	0.45		280	0.84
31	174	0.52	5000	0.45		284	0.85
32	174	0.52	5000	0.45		285	0.85
33	174	0.52	5000	0.45		264	0.79
34	174	0.52	5000	0.45		275	0.82
35	174	0.52	5000	0.45		291	0.87
36	174	0.52	5000	0.45		281	0.84
37	174	0.52	5000	0.45		284	0.85
38	174	0.52	5000	0.45		252	0.75
39	174	0.52	5000	0.45		270	0.81

continued on next page

continued from previous page

Test #	$\sigma_{applied}$ (MPa)	Fa	n	$\frac{n}{N}$	Premature failure	$X_{t,residual}$ (MPa)	Fr
40	174	0.52	5000	0.45		274	0.82
41	174	0.52	5000	0.45		255	0.76
42	174	0.52	5000	0.45		289	0.87
43	174	0.52	5000	0.45		275	0.82
44	174	0.52	5021	0.45	yes	0	0.00
45	174	0.52	5522	0.49	yes	0	0.00
46	174	0.52	6000	0.54		274	0.82
47	174	0.52	6000	0.54		290	0.87
48	174	0.52	6000	0.54		251	0.75
49	174	0.52	6000	0.54		288	0.86
50	174	0.52	6000	0.54		263	0.79
51	174	0.52	6000	0.54		253	0.76
52	174	0.52	6000	0.54		287	0.86
53	174	0.52	6000	0.54		283	0.85
54	174	0.52	6000	0.54		270	0.81
55	174	0.52	6000	0.54		250	0.75
56	174	0.52	5999	0.54	yes	0	0.00
57	174	0.52	7000	0.63		234	0.70
58	174	0.52	7000	0.63		285	0.85
59	174	0.52	7000	0.63		248	0.74
60	174	0.52	7000	0.63		264	0.79
61	174	0.52	7000	0.63		272	0.81
62	174	0.52	7000	0.63		270	0.81
63	174	0.52	7000	0.63		266	0.80
64	174	0.52	7000	0.63		257	0.77
65	174	0.52	7000	0.63		264	0.79
66	174	0.52	7000	0.63		241	0.72
67	174	0.52	7000	0.63		256	0.77
68	174	0.52	7000	0.63		271	0.81
69	174	0.52	7000	0.63		234	0.70
70	174	0.52	7000	0.63		259	0.77
71	174	0.52	7000	0.63		264	0.79
72	147	0.44	5000	0.11		302	0.90
73	147	0.44	5000	0.11		286	0.86
74	147	0.44	5000	0.11		268	0.80
75	147	0.44	5000	0.11		294	0.88
76	147	0.44	5000	0.11		289	0.87

continued on next page

continued from previous page

Test #	$\sigma_{applied}$ (MPa)	Fa	n	$\frac{n}{N}$	Premature failure	$X_{t,residual}$ (MPa)	Fr
77	147	0.44	5000	0.11		303	0.91
78	147	0.44	5000	0.11		299	0.90
79	147	0.44	5000	0.11		278	0.83
80	147	0.44	5000	0.11		272	0.82
81	147	0.44	5000	0.11		303	0.91
82	147	0.44	5000	0.11		307	0.92
83	147	0.44	5000	0.11		276	0.83
84	147	0.44	5000	0.11		286	0.86
85	147	0.44	5000	0.11		299	0.90
86	147	0.44	5000	0.11		322	0.96
87	147	0.44	15000	0.34		284	0.85
88	147	0.44	15000	0.34		281	0.84
89	147	0.44	15000	0.34		274	0.82
90	147	0.44	15000	0.34		268	0.80
91	147	0.44	15000	0.34		257	0.77
92	147	0.44	15000	0.34		288	0.86
93	147	0.44	15000	0.34		265	0.79
94	147	0.44	15000	0.34		263	0.79
95	147	0.44	15000	0.34		258	0.77
96	147	0.44	15000	0.34		227	0.68
97	147	0.44	22691	0.52	yes	0	0.00
98	147	0.44	25000	0.57		233	0.70
99	147	0.44	25000	0.57		280	0.84
100	147	0.44	25000	0.57		241	0.72
101	147	0.44	25000	0.57		265	0.79
102	147	0.44	25000	0.57		237	0.71
103	147	0.44	25000	0.57		269	0.81
104	147	0.44	25000	0.57		228	0.68
105	147	0.44	25000	0.57		254	0.76
106	147	0.44	25000	0.57		231	0.69
107	147	0.44	25000	0.57		277	0.83
108	147	0.44	25000	0.57		231	0.69
109	147	0.44	25000	0.57		248	0.74
110	147	0.44	25000	0.57		264	0.79
111	147	0.44	25000	0.57		249	0.75
112	147	0.44	25000	0.57		263	0.79
113	147	0.44	28110	0.64	yes	0	0.00

continued on next page

continued from previous page

Test #	$\sigma_{applied}$ (MPa)	Fa	n	$\frac{n}{N}$	Premature failure	$X_{t,residual}$ (MPa)	Fr
114	147	0.44	28376	0.64	yes	0	0.00
115	147	0.44	28945	0.66	yes	0	0.00
116	147	0.44	29813	0.68	yes	0	0.00
117	147	0.44	30000	0.68		255	0.76
118	147	0.44	30000	0.68		209	0.62
119	147	0.44	30000	0.68		252	0.75
120	147	0.44	30000	0.68		206	0.62
121	147	0.44	30000	0.68		266	0.80
122	147	0.44	30000	0.68		241	0.72
123	147	0.44	30000	0.68		243	0.73
124	147	0.44	30000	0.68		253	0.76
125	147	0.44	30000	0.68		210	0.63
126	147	0.44	30000	0.68		247	0.74
127	147	0.44	30615	0.70	yes	0	0.00
128	147	0.44	31938	0.73	yes	0	0.00
129	147	0.44	32861	0.75	yes	0	0.00
130	147	0.44	33238	0.76	yes	0	0.00
131	147	0.44	35000	0.80		261	0.78
132	147	0.44	35000	0.80		237	0.71
133	147	0.44	35000	0.80		202	0.60
134	147	0.44	35000	0.80		256	0.77
135	147	0.44	35000	0.80		166	0.50
136	147	0.44	35000	0.80		226	0.68
137	147	0.44	35000	0.80		277	0.83
138	147	0.44	35000	0.80		228	0.68
139	147	0.44	35000	0.80		245	0.73
140	147	0.44	35000	0.80		232	0.70
141	147	0.44	35000	0.80		250	0.75
142	147	0.44	35000	0.80		222	0.66
143	147	0.44	35000	0.80		215	0.64
144	147	0.44	35000	0.80		249	0.75
145	147	0.44	35000	0.80		209	0.62
146	120	0.36	50000	0.13		275	0.82
147	120	0.36	50000	0.13		296	0.89
148	120	0.36	50000	0.13		267	0.80
149	120	0.36	50000	0.13		281	0.84
150	120	0.36	50000	0.13		292	0.87

continued on next page

continued from previous page

Test #	$\sigma_{applied}$ (MPa)	Fa	n	$\frac{n}{N}$	Premature failure	$X_{t,residual}$ (MPa)	Fr
151	120	0.36	50000	0.13		263	0.79
152	120	0.36	50000	0.13		251	0.75
153	120	0.36	50000	0.13		268	0.80
154	120	0.36	50000	0.13		300	0.90
155	120	0.36	132716	0.35	yes	0	0.00
156	120	0.36	150000	0.40		250	0.75
157	120	0.36	150000	0.40		273	0.82
158	120	0.36	150000	0.40		277	0.83
159	120	0.36	150000	0.40		293	0.88
160	120	0.36	150000	0.40		279	0.84
161	120	0.36	150000	0.40		272	0.82
162	120	0.36	150000	0.40		277	0.83
163	120	0.36	150000	0.40		263	0.79
164	120	0.36	150000	0.40		269	0.81
165	120	0.36	150000	0.40		219	0.66
166	120	0.36	238369	0.63	yes	0	0.00
167	120	0.36	250000	0.66		231	0.69
168	120	0.36	250000	0.66		270	0.81
169	120	0.36	250000	0.66		250	0.75
170	120	0.36	250000	0.66		257	0.77
171	120	0.36	281382	0.75	yes	0	0.00
172	120	0.36	300000	0.80		249	0.75
173	120	0.36	300000	0.80		193	0.58
174	120	0.36	350000	0.93		206	0.62
175	120	0.36	350000	0.93		246	0.74
176	120	0.36	350000	0.93		231	0.69
177	120	0.36	350000	0.93		281	0.84
178	120	0.36	350000	0.93		190	0.57
179	120	0.36	350000	0.93		221	0.66
180	120	0.36	350000	0.93		237	0.71
181	120	0.36	350000	0.93		232	0.69
182	120	0.36	350000	0.93		262	0.78
183	120	0.36	350000	0.93		258	0.77
184	120	0.36	350000	0.93		240	0.72
185	120	0.36	350000	0.93		212	0.63
186	120	0.36	350000	0.93		174	0.52
187	100	0.3	2000000	-		235	0.70

continued on next page

continued from previous page

Test #	$\sigma_{applied}$ (MPa)	Fa	n	$\frac{n}{N}$	Premature failure	$X_{t,residual}$ (MPa)	Fr
188	84	0.25	10000000	-		265	0.79
189	84	0.25	10000000	-		294	0.88

4.7.4 Spectrum loading residual strength data

Table 4.10: Descending, highest to lowest, stress ordered 735641 cycle block loading spectrum residual strength results for VARTM E-glass/vinyl ester quasi-isotropic laminate subjected to fatigue at $R = 0.1$

Test #	$X_{t,residual}$ (MPa)	Fr
1	277	0.83
2	282	0.84
3	299	0.90
4	304	0.91
5	289	0.86
6	301	0.90
7	274	0.82
8	272	0.81
9	302	0.90
10	262	0.78
11	285	0.85

Table 4.11: Ascending, lowest to highest, stress ordered 735641 cycle block loading spectrum residual strength results for VARTM E-glass/vinyl ester quasi-isotropic laminate subjected to fatigue at $R = 0.1$

Test #	$X_{t,residual}$ (MPa)	Fr
1	312	0.94
2	287	0.86
3	302	0.91
4	288	0.86
5	274	0.82
6	289	0.87
7	302	0.90
8	293	0.88
9	260	0.78
10	272	0.81
11	299	0.90
12	297	0.89
13	269	0.81

Table 4.12: Random spectrum failure times and residual strength at failure for VARTM E-glass/vinyl ester quasi-isotropic laminate subjected to fatigue at $R = 0.1$

Test #	cycles to (MPa)	$X_{t,residual}$ at failure failure	Fr at failure
1	385223	-	-
2	213639	-	-
3	227764	163	0.49
4	389921	166	0.50
5	335291	150	0.45
6	290893	146	0.44
7	269404	163	0.49
8	202005	148	0.44
9	400860	164	0.49

continued on next page

continued from previous page

Test #	cycles to (MPa)	$X_{t,residual}$ at failure	Fr at failure
10	203809	163	0.49
11	204803	166	0.50
12	371406	155	0.47

Chapter 5

Conclusion

5.1 Summary of Results

This thesis presented the results for two statistical residual strength studies in E-glass/vinyl ester composites. These studies have been aimed at furthering a model that could be used to develop statistical design guidelines for the material system based on a limited amount of test data.

A non-linear residual strength model was applied to calculate residual strength distributions. These results are very positive for constant amplitude fatigue and worked well in the case of a ordered block loading spectrum. However, at this point, the mean or Weibull β values are based directly on curve fits to extensive similar data and thus do not present a true "prediction" technique. We do note that in general, the experimental residual strength distributions are narrower than those calculated using this model with the strength-life equal rank assumption. While this result is conservative, perhaps this assumption needs to be reevaluated for its relevance in predicting strength distributions during fatigue. Unfortunately, it is impossible to actually verify the strength-life assumption experimentally, so we will have to continue to rely on modeling results to assess it's accuracy.

In Chapter 4 we showed that the residual strength model failed to account for the much more rapid degradation of the material found under random ordered spectrum fatigue where there are frequent substantial changes in the fatigue load. This result is similar to previous studies of spectrum loading in composite materials presented in [27],[28],[15] ,[37], [14]. However, so far, no satisfactory explanation for this phenomenon exists and curve fitting "cycle-mix" concepts such as those presented by Schaff and Davidson [27] require very large amounts of data, especially if multiple stress ratios are to be considered. At this time, there is no published research that provides such a data set and applies it using this methodology.

An additional approach would be to use the residual stiffness degradation as a measure of the off axis damage in the laminate as we did in Chapter 3. This might produce more accurate results, but creates the additional problem of predicting the laminate modulus as a function of time under spectrum loading. So far, there is no good way to do this based on a curve fit or phenomenological approach. However, for successful optimized design with structural composites, some method must be developed that takes these effects into account.

In metallic materials, the focus has been on evaluation of crack growth under spectrum load conditions [33]. Perhaps a similar approach of modeling the damage on a micro-scale within the composite will have more success. The problem of a micro-mechanics approach to fatigue is complicated by the interaction of different lamina within the laminate that will have different fatigue failure modes and result in stress redistribution throughout the life of the composite.

5.2 Future Outlook

Based on the available information for fatigue of FRP composites under spectrum loading with frequent stress level changes, it is apparent that the current phenomenological residual strength models are inadequate. Adding additional factors to take cycle-mixing into account overly complicates the model application and requires large experimental data sets for each new material system, orientation, or loading. Thus, a micro-mechanics based modeling approach for fatigue that better interprets the effect of changes in loading stess level, stress ratio, etc. is desirable. Huang [18] published some work on developing such a model for unidirectional composites under cyclic loading in 2002 and the results were very promising in the graphite/epoxy and glass/epoxy lamina examined. The concept of a micro-mechanics model for fatigue has also been studied by Dzenis in [10] and [11] who developed a "stocastic mesomechanics modeling" approach to low cycle fatigue damage in graphite cross-ply laminates. Here non-destructive evaluation including acoustic emission was used to provide data for this model.

Unfortunately, the lamina and laminate mechanics become substantially more complex for woven composites. The most common static strength and stiffness micro-mechanics models for these materials are based on the "bridging" model [19] or authors simply resort to finite element analysis of a representative volume element. The bridging model concept using existing unidirectional material fatigue properties was applied to the case of bi-axial fatigue loading of woven composites by Huang [17] with reasonable results.

It is my belief that future efforts to improve residual strength models of composites subjected to random fatigue loading will need to be based on better understanding of the damage progression in the laminate. This will inherently involve micro-mechanics strength and stiffness models that account for the interaction of the lamina degradation and delimitation growth and can model each fatigue cycle loading and unloading so that the damage associated with random events can be included accurately. Statistical variation can potentially be included in these models or treated separately using Monte-Carlo simulations and strength-life equal rank type assumptions.

Bibliography

[1] RB Abernethy, JE Breneman, CH Medin, and GL Reinman. Weibull analysis handbook. Technical report, Pratt & Whitney Aircraft, 1983.

[2] T Adam, RF Dickson, CJ Jones, H Reiter, and B Harris. A power law fatigue damage model for fibre-reinforced plastic laminates. *Proc Instn Mech Engrs*, 200(C3):155–166, 1986.

[3] T Adam, N Gathercole, H Reiter, and B Harris. Life prediction for fatigue of t800/5245 carbon-firbre composites: I. constant amplitude loading. *Fatigue*, 16(8):533–547, 1994.

[4] LJ Broutman and S Sahu. A new theory to predict cumulative fatigue damage in fiberglass reinforced plastics. In *Composite Materials: Testing and Design (Second Conference) ASTEM STP 497*, pages 170–188. American Society for Testing and Materialss, 1972.

[5] PC Chou and R Croman. Residual strength in fatigue based on the strength-life equal rank assumption. *J. Composite Materials*, 12:177–194, 1978.

[6] X Diao, L Ye, and Y-W Mai. Statistical prediction of fatigue failure of fibre reinforced composite materials. *Applied Composite Materials*, 2:153–173, 1995.

[7] NE Dowling. Fatigue failure predictions for complicated stress-strain histories. *J. of Materials*, 7:71–87, 1972.

[8] NE Dowling. A review of fatigue life prediction methods. SAE Technical Paper Series 871966, SAE, 400 Commonwealth Drive, Warrendale, PA 15096, 1987.

[9] NE Dowling and S Thangjitham. An overview and discussion of basic methodolgy for fatigue. *Fatigue and Fracture Mechanics*, 31:3–31, 2001.

[10] YA Dzenis. Cycle-based analysis of damage and failure in advanced composites under fatigue 1. experimental observation of damage developement within. *Int. J. of Fatigue*, 25:499–510, 2003.

[11] YA Dzenis. Cycle-based analysis of damage and failure in advanced composites under fatigue 2. stochastic mesomechanics modeling. *Int. J. of Fatigue*, 25:511–520, 2003.

[12] BR Ellingwood. Load and resistance factor design for structures using fiber reinforced polymer composites. Technical Report NIST GCR 00-793, National Institute of Standards and Technology, 2000.

[13] BR Ellingwood. Toward load and resistance factor design for fiber reinforced polymer composites structures. *J. Structural Engineering*, 129:449–458, 2003.

[14] PAA Filis, IR Farrow, and IP Bond. Classical fatigue analysis and load cycle mix-event damage accumulation in fibre reinforced laminates. *Int. J. of Fatigue*, 26:565–573, 2004.

[15] N Garthercole, H Reiter, T Adam, and B Harris. Life prediction for fatigue of t800/5245 carbon-firbre composites: I. constant amplitude loading. *Fatigue*, 16(8):523–532, 1994.

[16] HT Hahn and RY Kim. Fatigue behavoir of composite laminate. *J. Composite Materials*, 10:156–180, 1976.

[17] ZM Huang. Fatigue life predition of a woven fabric composite subjected to biaxial cyclic loads. *Composites: Part A*, 33:253–266, 2002.

[18] ZM Huang. Micromechanical modeling of fatigue strength of unidirectional fibrous composites. *Int. J. of Fatigue*, 24:659–670, 2002.

[19] ZM Huang and S Ramakrishna. Modeling inelastic and strength properties of textile laminates: a unified approach. *Composites Science and Technology*, 63:445–466, 2003.

[20] W Hwang and KS Han. Cumulative damage models and multi-stress fatigue life prediction. *J. Composite Materials*, 20:125–153, 1986.

[21] MA Miner. Cumulative damage in fatigue. *J. Applied Mechanics*, 67:A159–A164, 1945.

[22] W Van Paepegem and J Degrieck. Effects of load sequence and block loading on the fatigue response of fiber-reinforced composites. *J. Mech. of Adv. Materials and Structures*, 9:19–35, 2002.

[23] P Papanikos, KI Tserpes, and S Pantelakis. Modelling of fatigue damage progression and life of cfrp laminates. *Fatigue & Fractures of Eng. Mat. & Struct.*, 26(1):37–47, 2003.

[24] KL Reifsnider, editor. *Fatigue of Composite Materials*. Composite Materials Series v. 4. Elsevier, New York, 1991.

[25] KL Reifsnider and SW Case. *Damage Tolerance and Durability in Material Systems*. John Wiley & Sons, New York, 2002.

[26] A Rotem and HG Nelson. Residual strength of composite laminate subjected to tensile-compressive fatigue loading. *J. of Composites Technology & Research*, 12(2):76–84, 1990.

[27] JR Schaff and BD Davidson. Life prediction methodology for composite structures. part i - constant amplitude and two-stress level fatigue. *J. of Composite Materials*, 31(2):128–157, 1997.

[28] JR Schaff and BD Davidson. Life prediction methodology for composite structures. part ii - spectrum fatigue. *J. of Composite Materials*, 31(2):158–181, 1997.

[29] J Schön and A Blom. Fatigue life prediction and load cycle elimination during spectrum loading of composites. *International Journal of Fatigue*, 24:361–367, 2002.

[30] D Schultz and JJ Gerharz. Fatigue strength of a fibre-reinforced material. *Composites*, 8(4):245–249, 1977.

[31] D Schultz and JJ Gerharz. Fatigue strength of a fibre-reinforced material. *Composites*, 8(4):254–250, 1977.

[32] R Speckart, Nov. 2005. Personal Communication.

[33] R Sunder. Spectrum load fatigue-underlying mechanisms and their significance in testing and analysis. *Int. J. of Fatigue*, 25:971–981, 2003.

[34] R Talreja. *Fatigue of Composite Materialss*, chapter Fatigue of composite materials: damage mechanisms and fatigue-life diagrams. Technomic, Lancaster, PA, 1987.

[35] R Talreja. Internal variable damage mechanics of composite materials. In J P Bochler, editor, *Yielding, Damage, and Fatigue of Anisotropic Solids, EGF5*, pages 509–533, London, 1990. Mechanical Engineering Publications.

[36] N Wahl, D Samborsky, J Mandell, and D Cairns. Spectrum fatigue lifetime and residual strength for fiberglass laminates in tension. In *ASME Wind Energy Symposium*, AIAA-2001-0025, pages 1–11. AIAA, 2001.

[37] NK Wahl. *Spectrum Fatigue Lifetime and Residual Strength for Fiberglass Laminates*. PhD thesis, Department of Mechanical Engineering, Montana State University, August 2001.

[38] W Weibull. A statistical distribution fuction of wide applicability. *J. Applied Mechanics*, pages 293–297, 1951.

[39] HA Whitworth. Modeling stiffness reduction of graphite/epoxy composite laminates. *J. Composite Materials*, 21:362–372, 1987.

[40] J Yang. Fatigue and residual strength degradation for graphite/epoxy composites under tension-compression cyclic loadings. *J. Composite Materials*, 12:19–39, 1978.

[41] JN Yang and S Du. An exploratory study into the fatigue of composites under spectrum loading. *J. Composite Materials*, 17(511-526), 1983.

[42] JN Yang and DL Jones. Effect of load sequence on the statistical fatigue of composites. *AIAA Journal*, 12:1525–1531, 1980.

[43] JN Yang and MD Liu. Residual strength degradation model and theory of periodic proof tests for graphite/epoxy laminates. *J. Composite Materials*, 11:176–203, 1977.

[44] JN Yang, HS Yang, and DL Jones. A stiffness-based statistical model for predicting the fatigue life of graphite/epoxy laminates. *J. Composites Technology & Research*, 11(4):129–134, 1989.

Vita

Nathan grew up in central Vermont. He was home-schooled prior to attending Vermont Technical College in place of his senior year of high-school. In 2003, Nathan received a Bachelors of Science with University Honors degree in Mechanical Engineering from Clarkson University, Potsdam NY. Following this, he enrolled at Virginia Tech as a doctoral student in the Engineering Science and Mechanics Department. Nathan's interests and hobbies outside of his academic research include sailing, contra dance and country waltzing, skiing, bicycling, and environmental philosophy.